SECURITY INFORMATION

NACA

RESEARCH MEMORANDUM

for the

U. S. Air Force

STABILITY AND CONTROL CHARACTERISTICS AT LOW SPEED OF A MODIFIED 1/10-SCALE MODEL OF THE MX-1554A DESIGN

By Vernard E. Lockwood and Martin Solomon

Langley Aeronautical Laboratory
Langley Field, Va.

CLASSIFIED DOCUMENT

This material contains information affecting the National Defense of the United States within the meaning of the espionage laws, Title 18, U.S.C., Secs. 793 and 794, the transmission or revelation of which in any manner to an unauthorized person is prohibited by law.

NATIONAL ADVISORY COMMITTEE
FOR AERONAUTICS

WASHINGTON

NACA RM SL53K25

NATIONAL ADVISORY COMMITTEE FOR AERONAUTICS

RESEARCH MEMORANDUM

for the

U. S. Air Force

STABILITY AND CONTROL CHARACTERISTICS AT LOW SPEED OF A MODIFIED 1/10-SCALE MODEL OF THE MX-1554A DESIGN

By Vernard E. Lockwood and Martin Solomon

SUMMARY

An investigation was made of the low-speed stability and control characteristics of a modified 1/10-scale model of the MX-1554A design. This design employs a triangular wing and triangular stabilizing surfaces.

The present paper contains the test results of a stability and control investigation of a model configuration designed to give more satisfactory stability and control than the configuration which was reported in NACA RM SL53A05. The modifications to the model included an increase in slotted-flap span, a redesigned tip aileron, fuselage tail cone, and speed brakes. This paper also includes the results of tests to determine:

(1) The effect of flow-control devices (leading-edge notches, fences, and chord-extensions) on the longitudinal stability and control.

(2) The effect of tank and pylon location on the longitudinal stability and control.

(3) The effect of a ground board on the longitudinal stability and control characteristics.

(4) The rotary stability derivatives.

(5) The effects of the model single support strut on the aerodynamic characteristics (tare corrections).

INTRODUCTION

An investigation of the stability and control characteristics at low speed of a modified 1/10-scale model of the MX-1554A design has been conducted in the Langley 300 MPH 7- by 10-foot tunnel. A previous investigation of the model at low speed (ref. 1) indicated the desirability of modifying the design to improve the lift and the stability and control characteristics. The modifications to the model included increasing the flap span to obtain greater lift at low angles of attack, redesigning of the tip aileron to increase lateral control, refairing of the rear end of the fuselage, and redesigning the speed brake to lessen interference with the horizontal stabilizer and to increase the drag. The lateral-control investigation was conducted in the Langley stability tunnel because it was thought greater accuracy could be obtained for this phase of the investigation.

The present paper contains the results of an investigation which is primarily one of longitudinal stability and control; however, some lateral stability and control results are included. The investigation includes determining a flap deflection which would provide maximum lift and stability in an angle-of-attack range of landing and take-off. Tests were conducted to determine the effects of tanks and speed brakes on the characteristics.

During the first series of tests, certain deficiencies were noted for the deflected-flaps configuration which necessitated broadening of the scope of the investigation. Various auxiliary flow control devices, such as chord-extensions, leading-edge notches, and flow fences, were used in several combinations in an attempt to increase the longitudinal stability. Some of these configurations were tested in the presence of a ground board to determine the effects at simulated landing and take-off conditions. The lateral-control tests conducted in the Langley stability tunnel utilized the circular test section and, therefore, the equipment was available for determining the rotary-stability derivatives which are included in this paper. A tare study was conducted to determine the effect on the aerodynamic characteristics of the model single support strut, the results of which are contained herein.

COEFFICIENTS AND SYMBOLS

All data are referred to the stability axes as indicated in figure 1. A point of 35 percent of the wing mean aerodynamic chord was used as center of moments. The coefficients and symbols used in this paper are defined as follows:

[redacted]

C_L	lift coefficient, Lift/qS
C_X	longitudinal-force coefficient, X/qS
C_Y	lateral-force coefficient, Y/qS
C_l	rolling-moment coefficient, L/qSb
C_m	pitching-moment coefficient, M/qS$\bar{c}$
C_n	yawing-moment coefficient, N/qSb
X	longitudinal force along X-axis, lb
Y	lateral force along Y-axis, lb
Z	force along Z-axis (lift equals -Z), lb
L	rolling moment about X-axis, ft-lb
M	pitching moment about Y-axis, ft-lb
N	yawing moment about Z-axis, ft-lb
q	free-stream dynamic pressure, $\frac{\rho V^2}{2}$, lb/sq ft
S	wing area, sq ft
$\bar{c}$	wing mean aerodynamic chord, ft
b	wing span, ft
V	free-stream velocity, ft/sec
ρ	mass density of air, slugs/cu ft
α	angle of attack of fuselage reference line, deg
i	angle of incidence of wing or stabilizer with respect to fuselage reference line, deg
δ	control-surface deflection in a plane perpendicular to hinge line, deg

[redacted]

H height of center of gravity of model above ground board based at $\alpha = 0^{\circ}$, in.

β angle of sideslip, deg

$C_{l_\beta} = \frac{\partial C_l}{\partial \beta}$

$C_{n_\beta} = \frac{\partial C_n}{\partial \beta}$ } lateral-stability parameters

$C_{Y_\beta} = \frac{\partial C_Y}{\partial \beta}$

pb/2V helix angle generated by wing tip in roll, radians

p rolling angular velocity, radians/sec

$C_{l_p} = \frac{\partial C_l}{\partial \frac{pb}{2V}}$

$C_{Y_p} = \frac{\partial C_Y}{\partial \frac{pb}{2V}}$ } rotary-stability derivatives

$C_{n_p} = \frac{\partial C_n}{\partial \frac{pb}{2V}}$

Subscripts:

a aileron

f flap

r rudder

t horizontal stabilizer

w wing

R right

[redacted]

Special notations:

Configuration

F	fuselage
W	wing
V	vertical fin
H	horizontal stabilizer

Fences

A, B, C, D, E	designation (fig. 3)
33, 46, 55, 64	location, percent b/2

APPARATUS AND METHODS

The model used in the present investigation was a modified 1/10-scale model of the MX-1554A design. The wing and stabilizing surfaces have delta plan forms with a small amount of sweepback of the trailing edges. The geometric characteristics of this model are presented in figure 2. The horizontal stabilizer was constructed with special fittings to allow testing as an all-movable surface. The location of the pivot was 65 percent of the mean aerodynamic chord of the horizontal tail.

Several air-flow control devices to alleviate longitudinal instability were tested; these include notches, chord-extensions, and fences. The geometry of these devices is given in figure 3.

A drawing showing the extent of the tail cone modification as compared with the previous one is given in figure 4.

The model had no internal ducting leading from the air scoop. To delay separation which would ordinarily occur from the sharp edges of the scoop, modeling clay was used to refair the throat and edges.

The model was also tested with wing tanks, landing gear, and modified speed brakes as shown in figure 2. The speed brakes were designed so that when they were deflected a large cutout appeared in the fuselage to allow air to flow about the inboard end of the brakes (fig. 2).

A ground board was used to simulate the airplane in the presence of the ground. The relative position of the model and the board is shown in figure 2.

[redacted]

In order to determine the interference effects of the single support strut, the model was inverted and a dummy strut attached to it. By testing the model with and without the dummy strut, the tare and interference effects could be determined.

Unless otherwise stated in the legends of the figures, the model configuration with the flaps deflected consisted of the landing gear extended with the main-landing-gear doors closed and the nose-gear door open. With the flaps retracted, the main landing gear and the nose gear were retracted and all doors were closed.

TESTS

The tests were conducted in the Langley 300 MPH 7- by 10-foot tunnel at the approximate conditions given in the following table:

Ground board	Dynamic pressure, lb/sq ft	Mach number	Reynolds number (a)
None	25.0	0.131	1,400,000
None	49.0	.183	1,840,000
None	83.4	.241	2,360,000
H = $12\frac{1}{2}$ in.	52.5	.189	1,870,000
None	100.1	.266	2,590,000

[a]The Reynolds number is based on a wing mean aerodynamic chord of 17.93 inches.

Several tests were conducted in the Langley stability tunnel, utilizing a circular test section. The approximate conditions for these tests were a dynamic pressure of 41 lb/sq ft corresponding to a Mach number of 0.167 and a Reynolds number of 1,650,000. By means of special equipment in the Langley stability tunnel enabling the airstream to be rotated at several known angular velocities, a series of tests were performed at values of $pb/2V$ of ± 0.0535, ± 0.0360, and ± 0.0178 radian.

CORRECTIONS

The angle of attack and drag have been corrected for jet-boundary effects computed on the basis of unswept wings by the method of reference 2. The correction to pitching moment due to tunnel induced upwash at the tail was found to be negligible.

[redacted]

Tare corrections from the model single support strut were not applied to the data but are presented in figure 5. These corrections should be applied as follows:

$$C_{L_c} = C_L - \Delta C_L$$

$$C_{X_c} = C_X - \Delta C_X$$

$$C_{m_c} = C_m - \Delta C_m$$

$$C_{l_{\beta_c}} = C_{l_\beta} - \Delta C_{l_\beta}$$

$$C_{Y_{\beta_c}} = C_{Y_\beta} - \Delta C_{Y_\beta}$$

$$C_{n_{\beta_c}} = C_{n_\beta} - \Delta C_{n_\beta}$$

where the subscript c refers to the corrected value of the coefficient and the coefficient without a subscript refers to the data presented herein. These tare corrections may also be applied to the data presented in reference 1. These tare corrections can probably be used for other stabilizer incidences but they are probably not reliable for tail-off configurations (horizontal or vertical) as the rear end of the fuselage was in the wake of the support strut fairing at high angles of attack. The tare tests were made at a dynamic pressure of 49 lb/sq ft; the results should apply, however, to any of the dynamic pressures used in this or the previous investigation of reference 1. The configurations of the model for the tare tests were:

(a) $\delta_f = 0^\circ$; Configuration FWVH, small notch fence E-33, all landing gear retracted and doors closed, and $i_t = -9.9^\circ$

(b) $\delta_f = 50^\circ$; Configuration FWVH, small notch, fence E-33, all landing gear extended with nose-gear door and top main-landing-gear doors open, and $i_t = -9.9^\circ$

Corrections have been applied to the data resulting from tunnel air-flow misalinement, and longitudinal-pressure gradient in the tunnel.

[redacted]

PRESENTATION OF RESULTS

In order to facilitate earlier publication of this paper, no analysis of results or conclusions have been attempted. However, this paper contains all the pertinent results of the present investigation of the MX-1554A design model and the results are presented in the following manner:

[redacted]

Langley Aeronautical Laboratory,
National Advisory Committee for Aeronautics,
Langley Field, Va., November 9, 1953.

Vernard E. Lockwood
Aeronautical Research Scientist

Martin Solomon
Aeronautical Research Scientist

Approved: Thomas A. Harris

Thomas A. Harris
Chief of Stability Research Division

ecc

REFERENCES

1. Lockwood, Vernard E., and Solomon, Martin: Stability and Control Characteristics at Low Speed of a 1/10-Scale Model of MX-1554A Design. NACA RM SL53A05, U. S. Air Force, 1953.

2. Gillis, Clarence L., Polhamus, Edward C., and Gray, Joseph L., Jr.: Charts for Determining Jet-Boundary Corrections for Complete Models in 7- by 10-Foot Closed Rectangular Wind Tunnels. NACA WR L-123, 1945. (Formerly NACA ARR L5G31.)

[redacted]

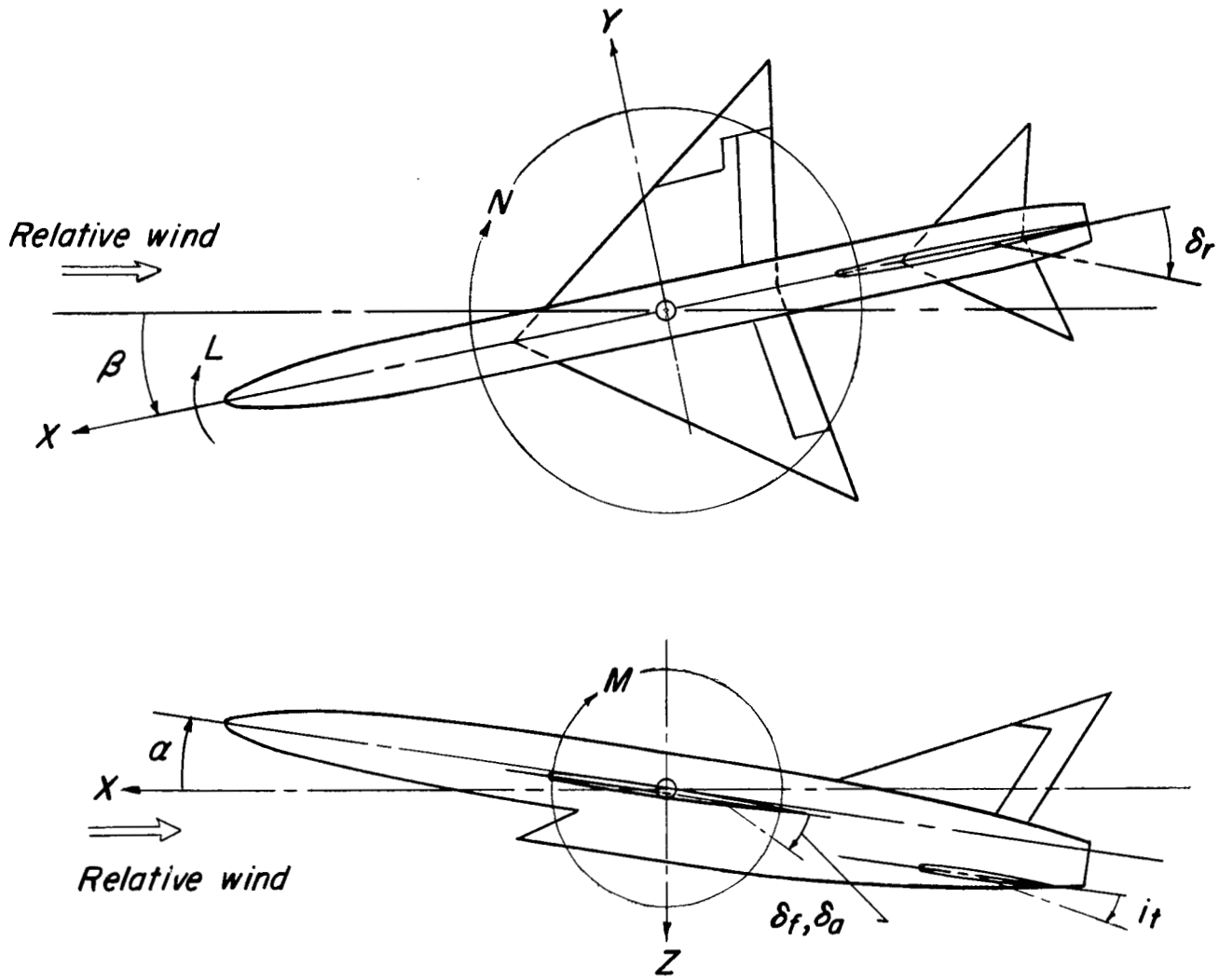

Figure 1.- System of axes and control-surface deflections. Positive directions of forces, moments, and angles are indicated by arrows.

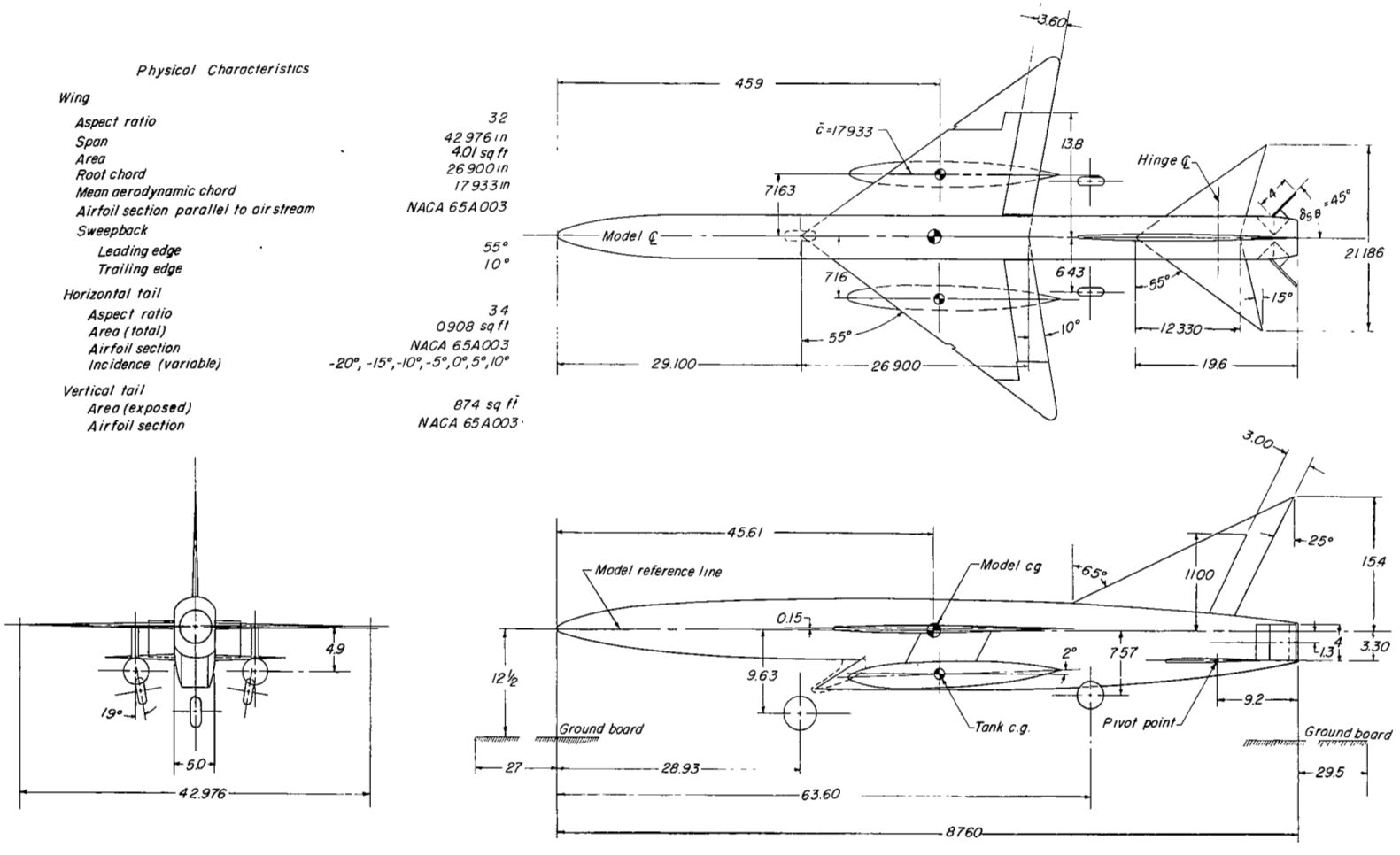

Figure 2.- Three-view drawing of model tested. All dimensions are in inches unless otherwise noted.

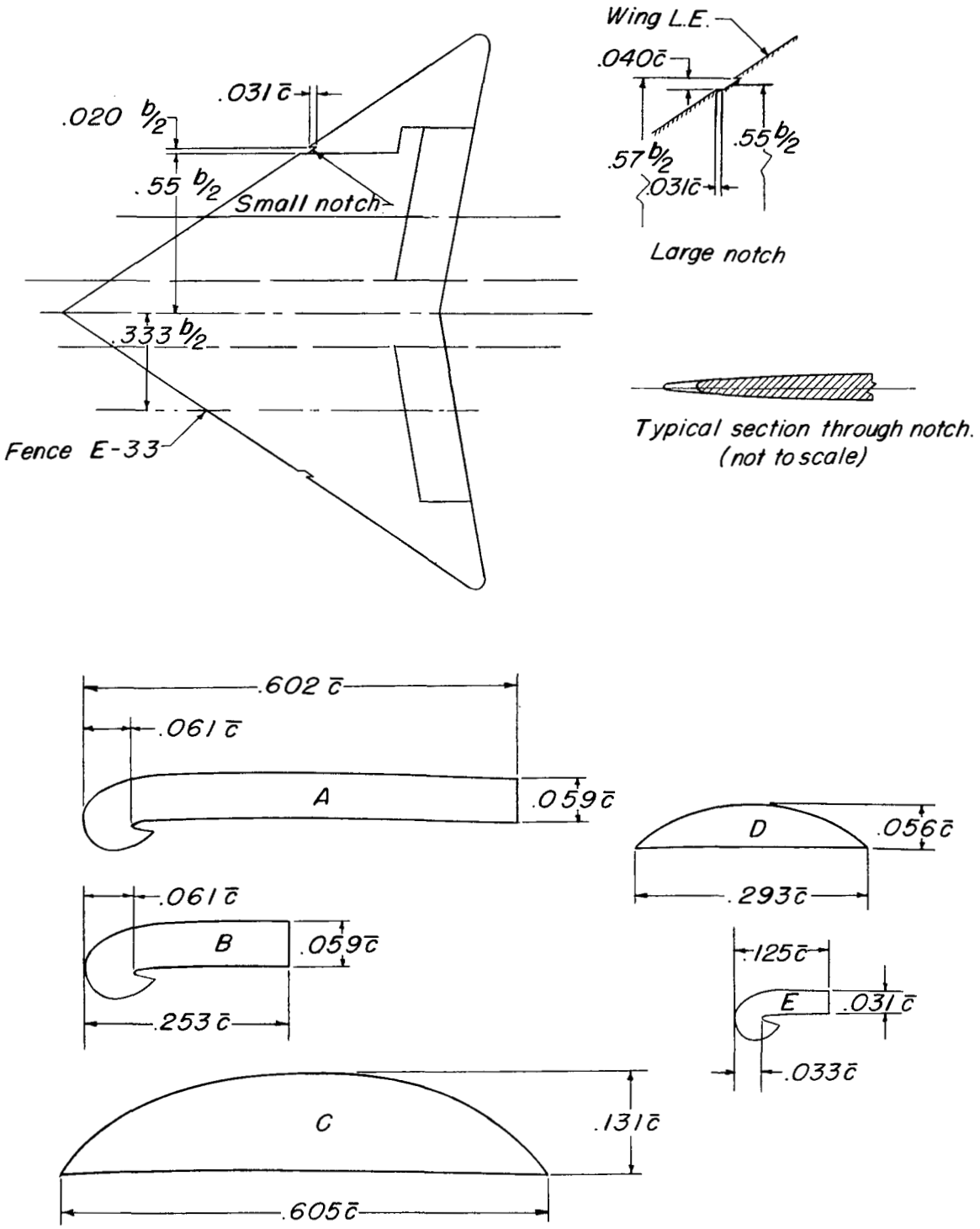

Figure 3.- Auxiliary flow control devices used (notches, fences, and chord-extensions).

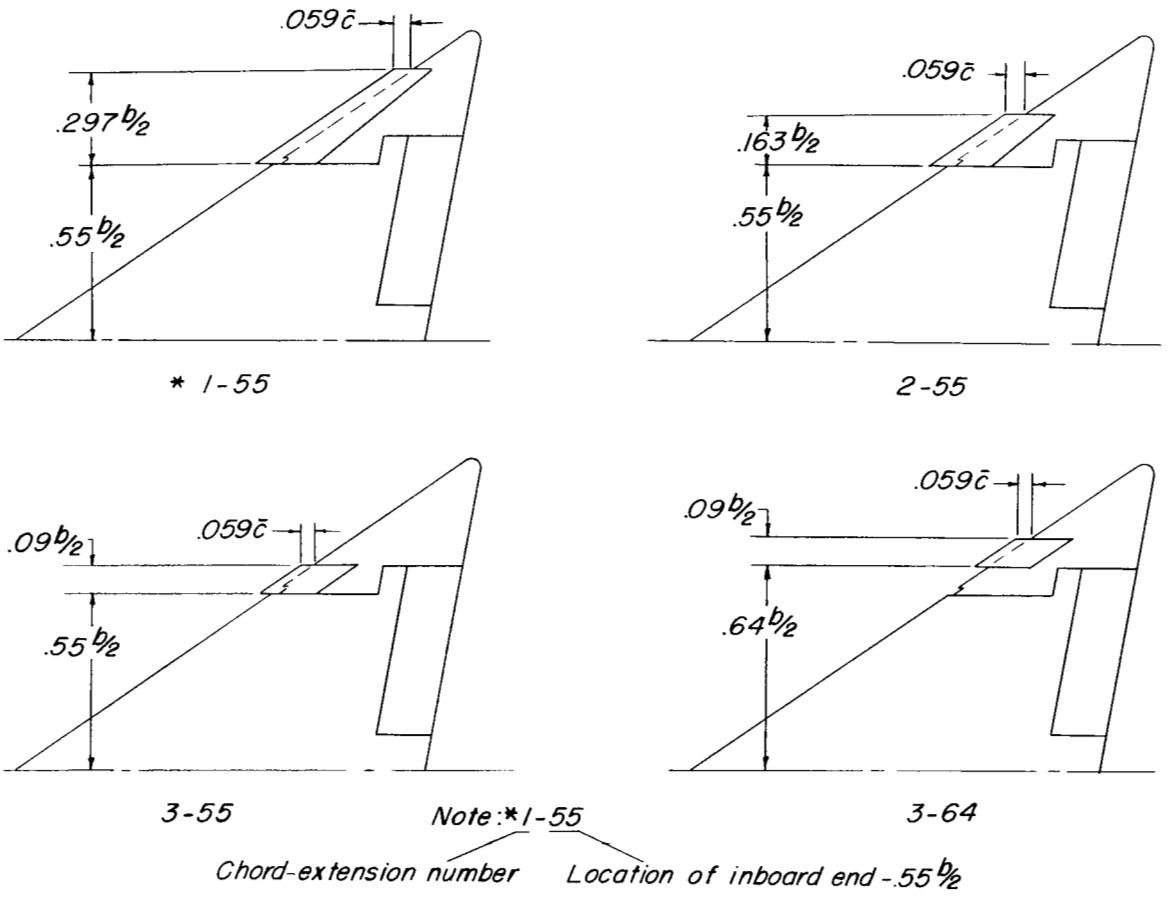

Typical section through chord-extension
(not to scale)

Figure 3.- Concluded.

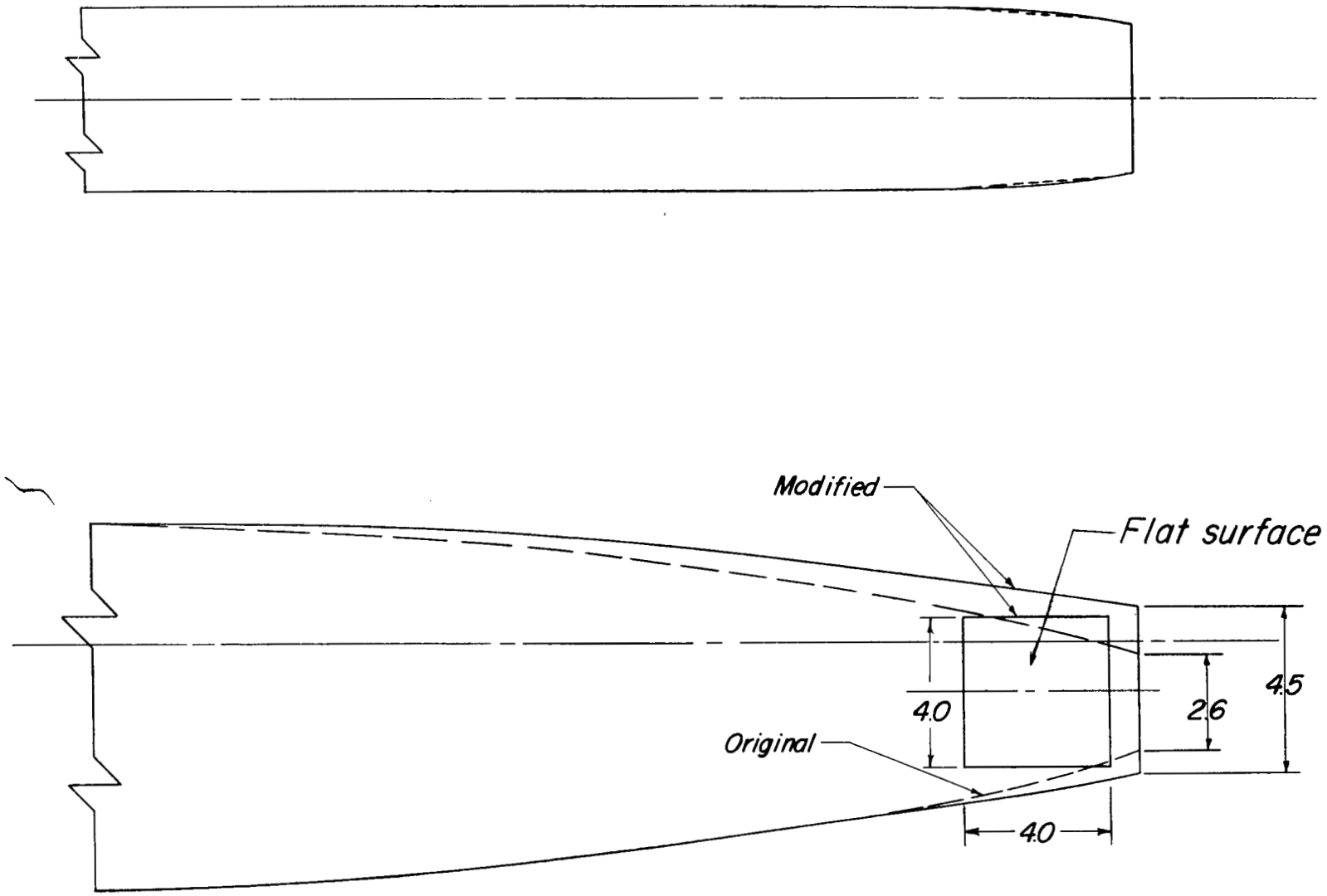

Figure 4.- Diagram of fuselage modification. All dimensions are in inches.

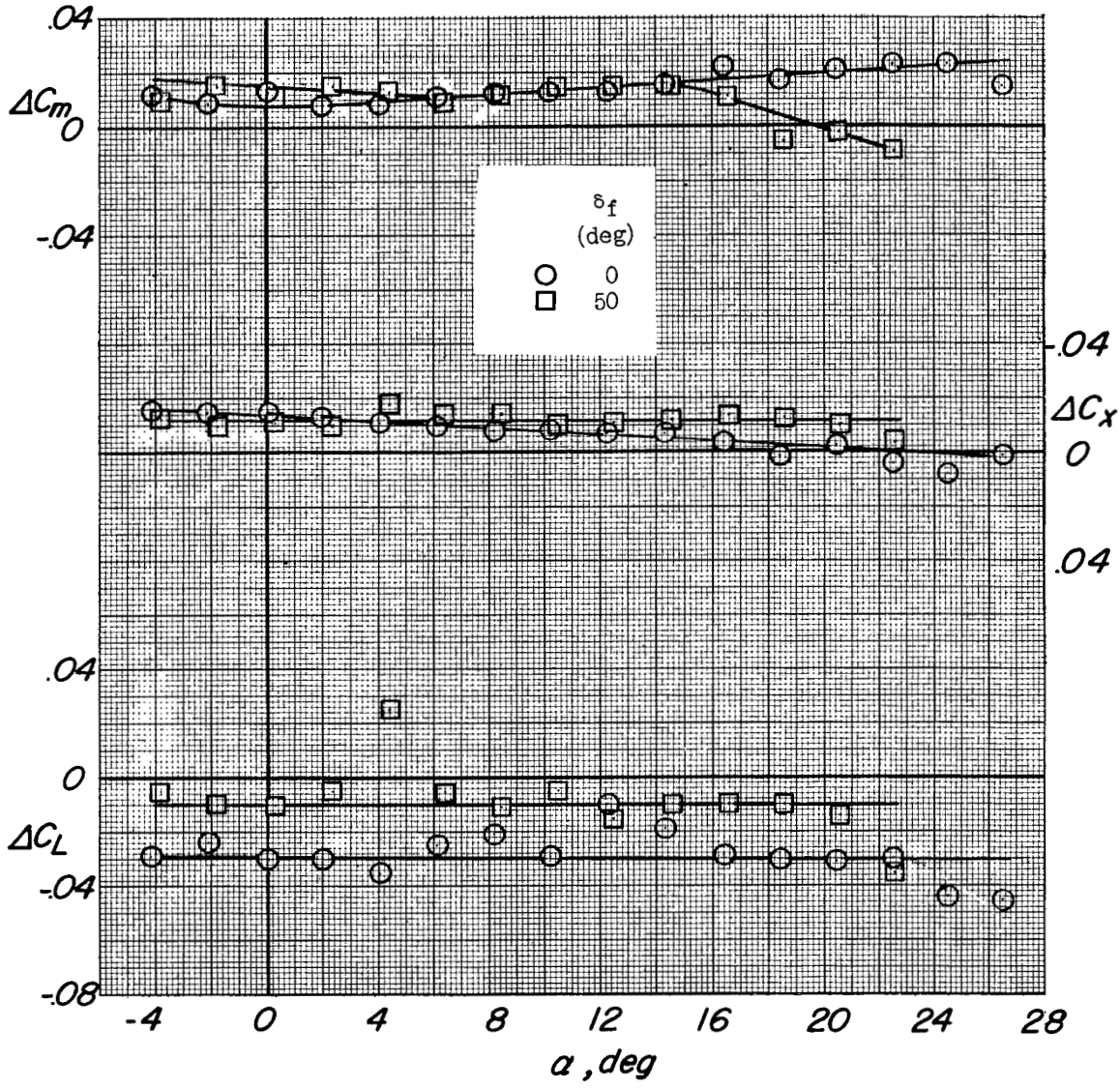

Figure 5.- The tare corrections to be applied to the data from the 1/10-scale model of the MX-1554A in the Langley 300 MPH 7- by 10-foot tunnel due to the interference of the single support strut. Configuration FWVH; $i_w = 0^o$; $i_t = -9.9^o$; small notch; fence E-33; q = 49 lb/sq ft.

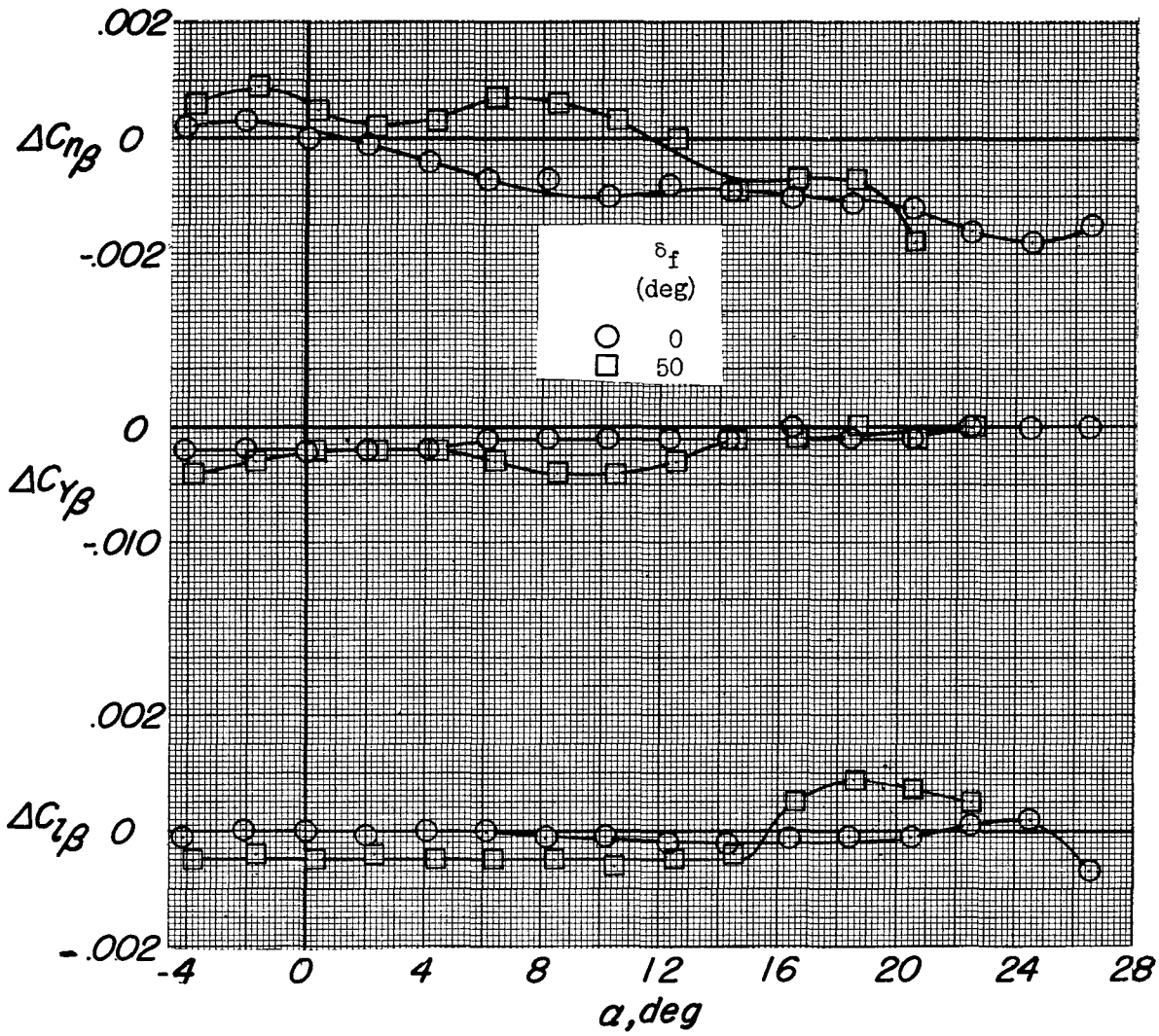

Figure 5.- Concluded.

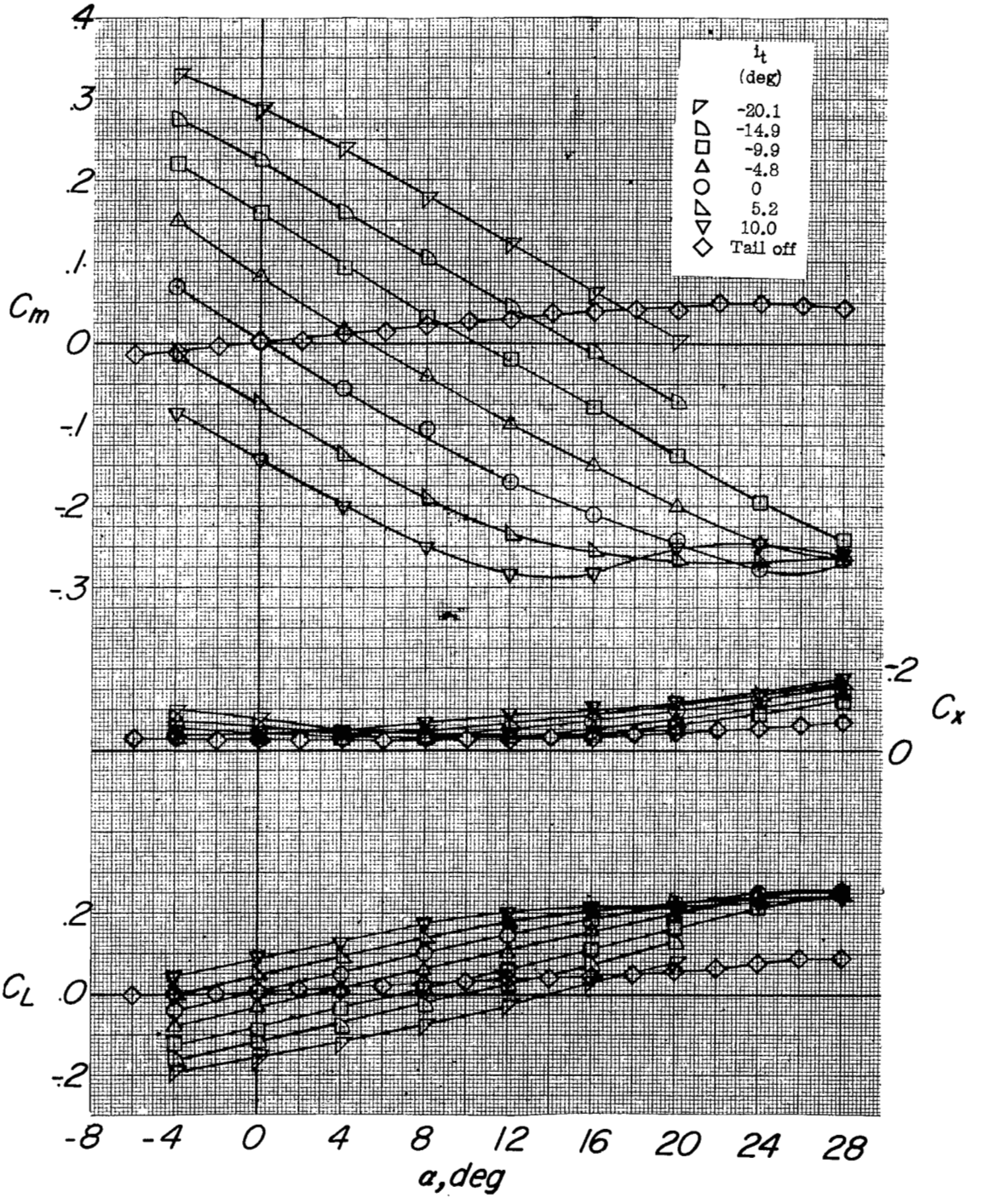

Figure 6.- The effect of the horizontal stabilizer on the aerodynamic characteristics in pitch. Configuration FH; q = 49 lb/sq ft.

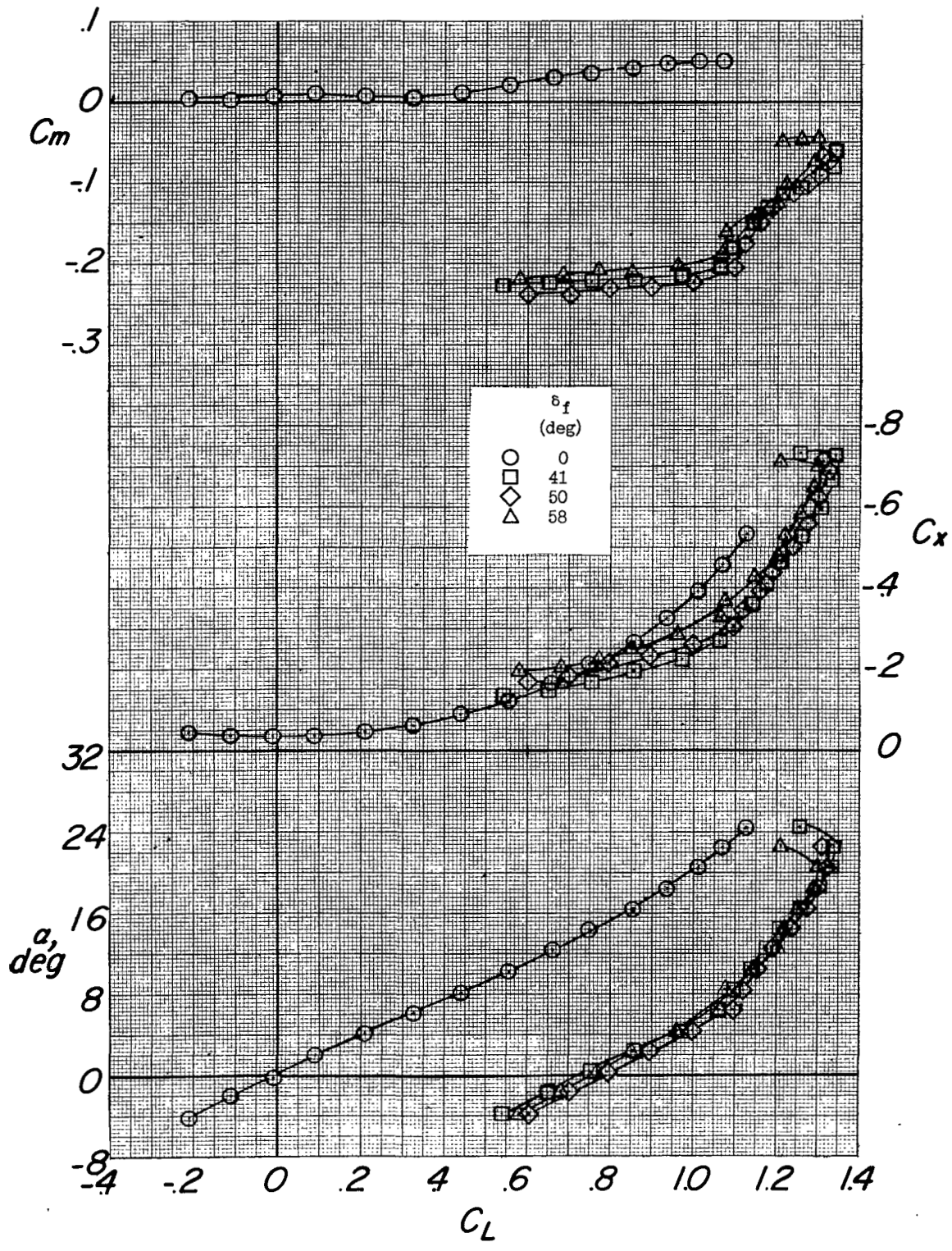

Figure 7.- The effect of flap deflection on the aerodynamic characteristics in pitch. Configuration FW; $i_w = 0^o$; landing gear off; q = 49 lb/sq ft.

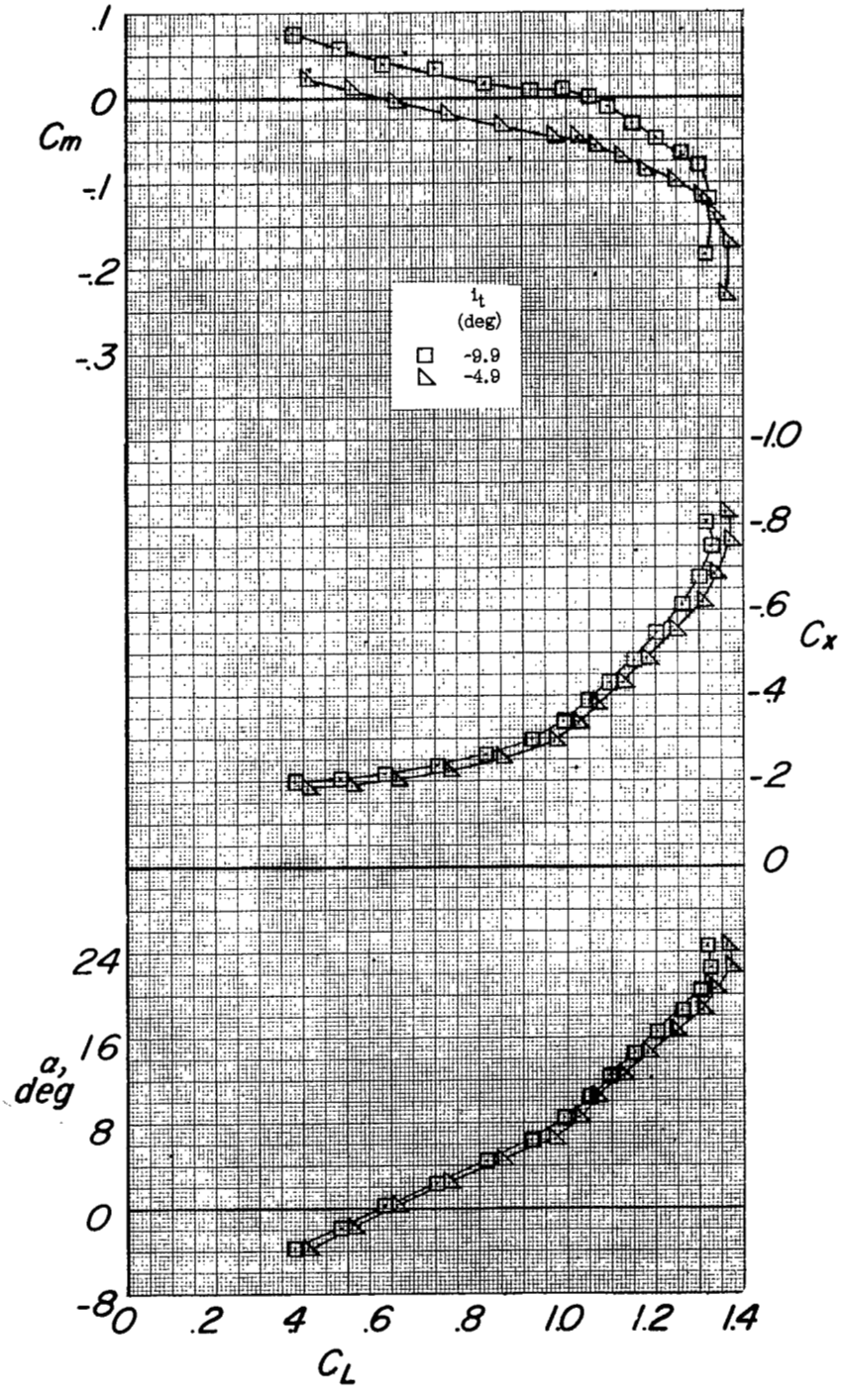

(a) $\delta_f = 43^\circ$.

Figure 8.- The effect of the horizontal stabilizer on the aerodynamic characteristics in pitch. Configuration FWVH; $i_w = 0^\circ$; q = 49 lb/sq ft.

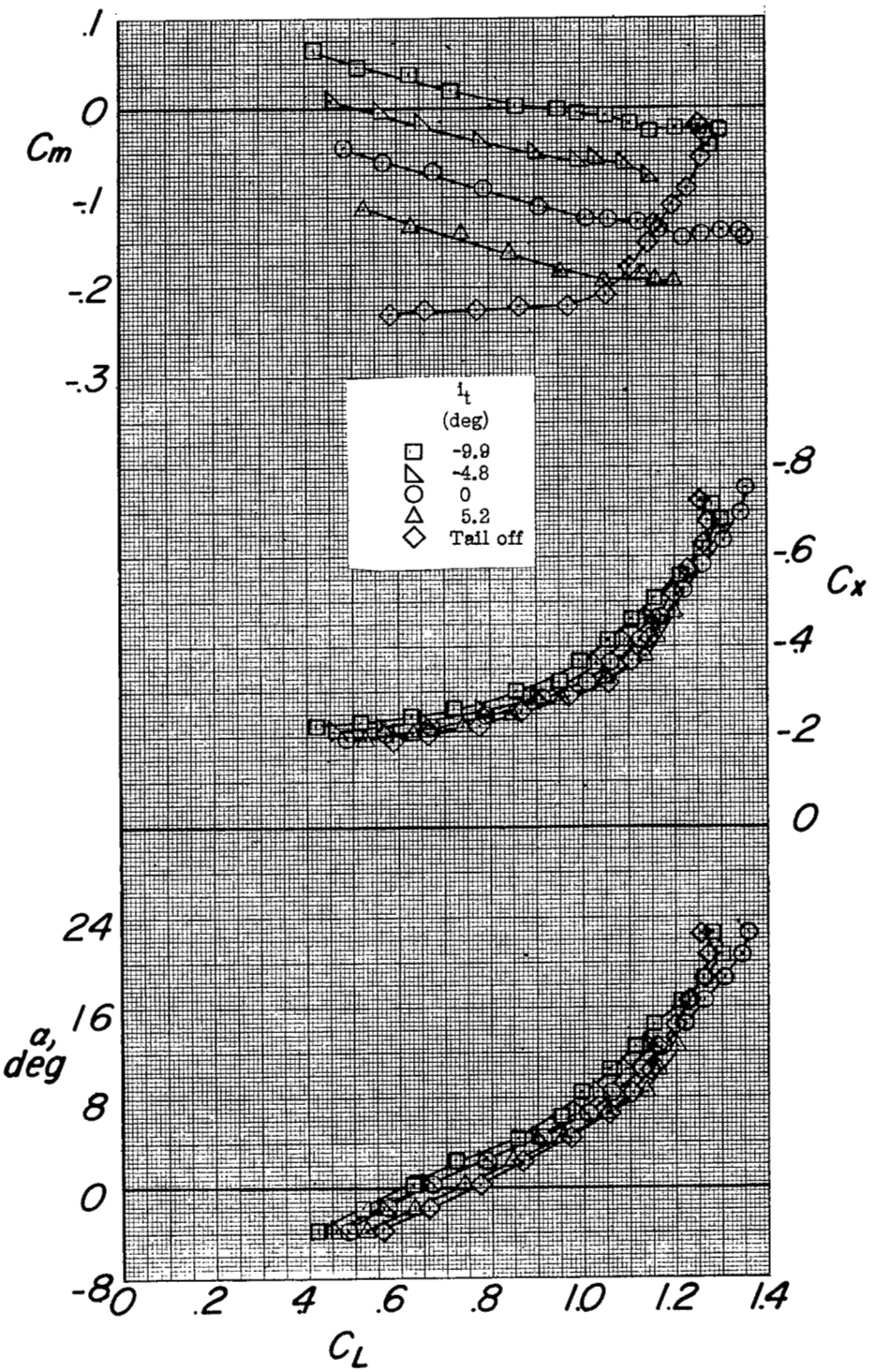

(b) $\delta_f = 50^\circ$.

Figure 8.- Continued.

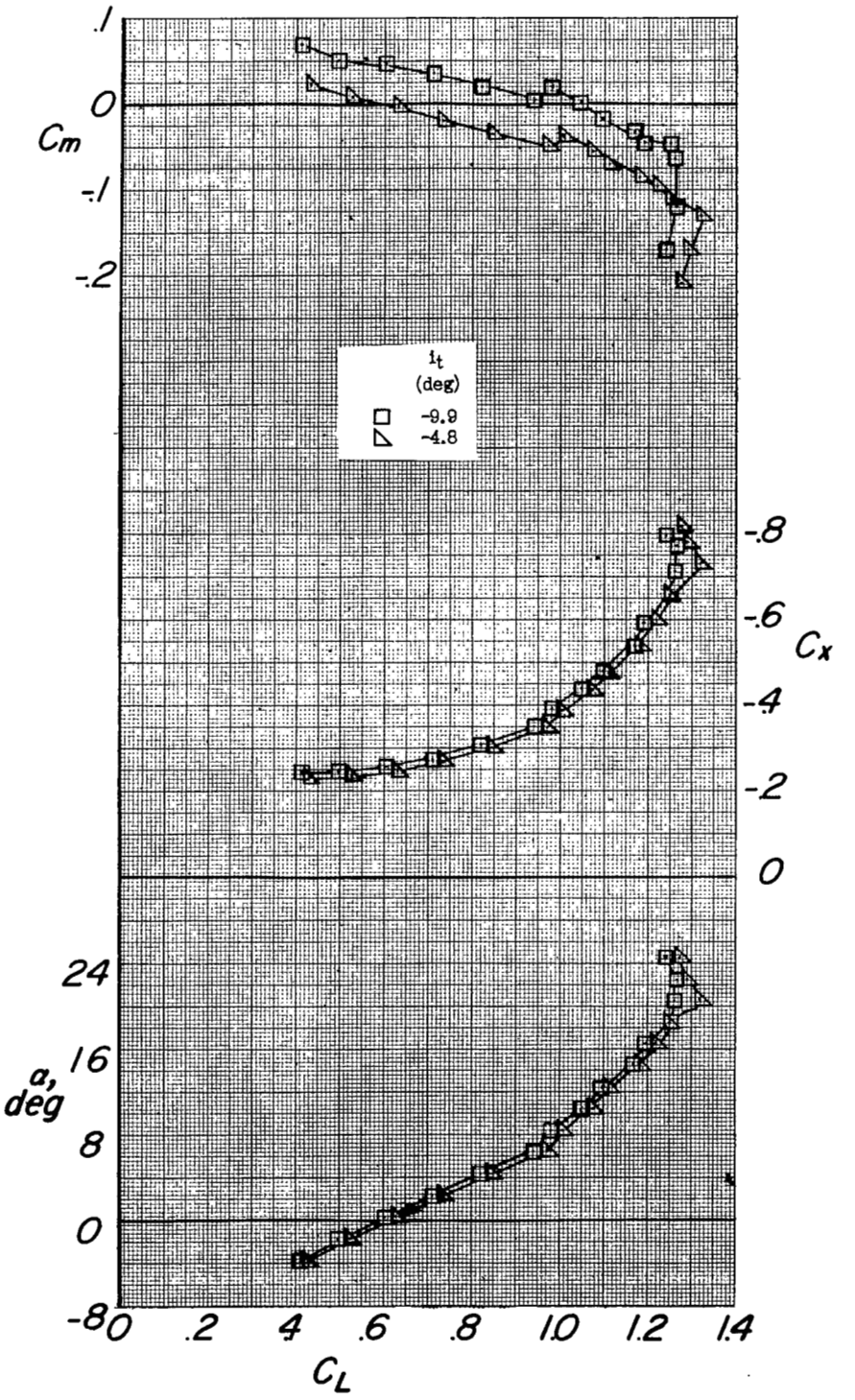

(c) $\delta_f = 58^\circ$.

Figure 8.- Concluded.

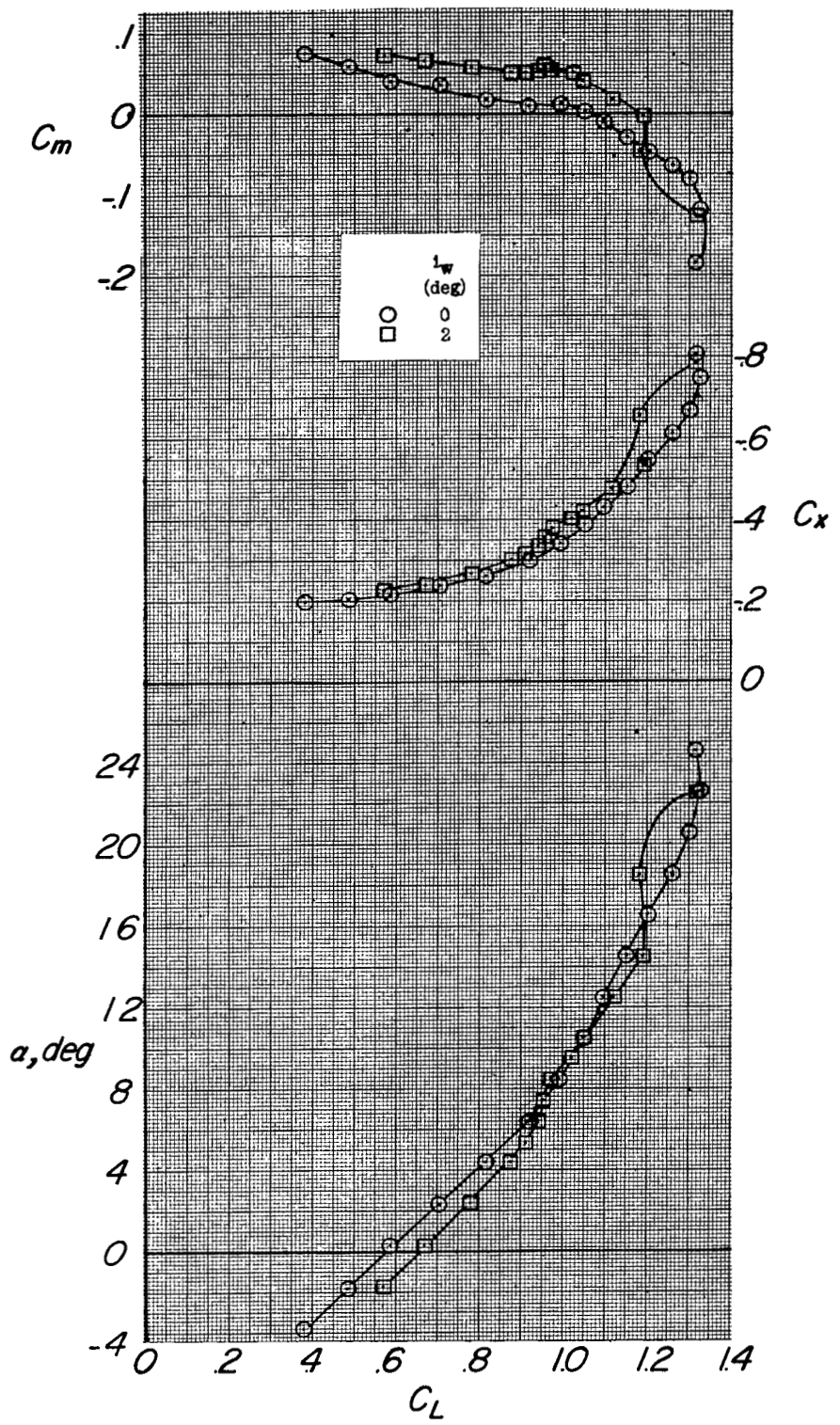

Figure 9.- The effect of wing incidence on the aerodynamic characteristics in pitch. Configuration FWVH; $\delta_f = 43^\circ$; $i_t = -9.9^\circ$; q = 49 lb/sq ft.

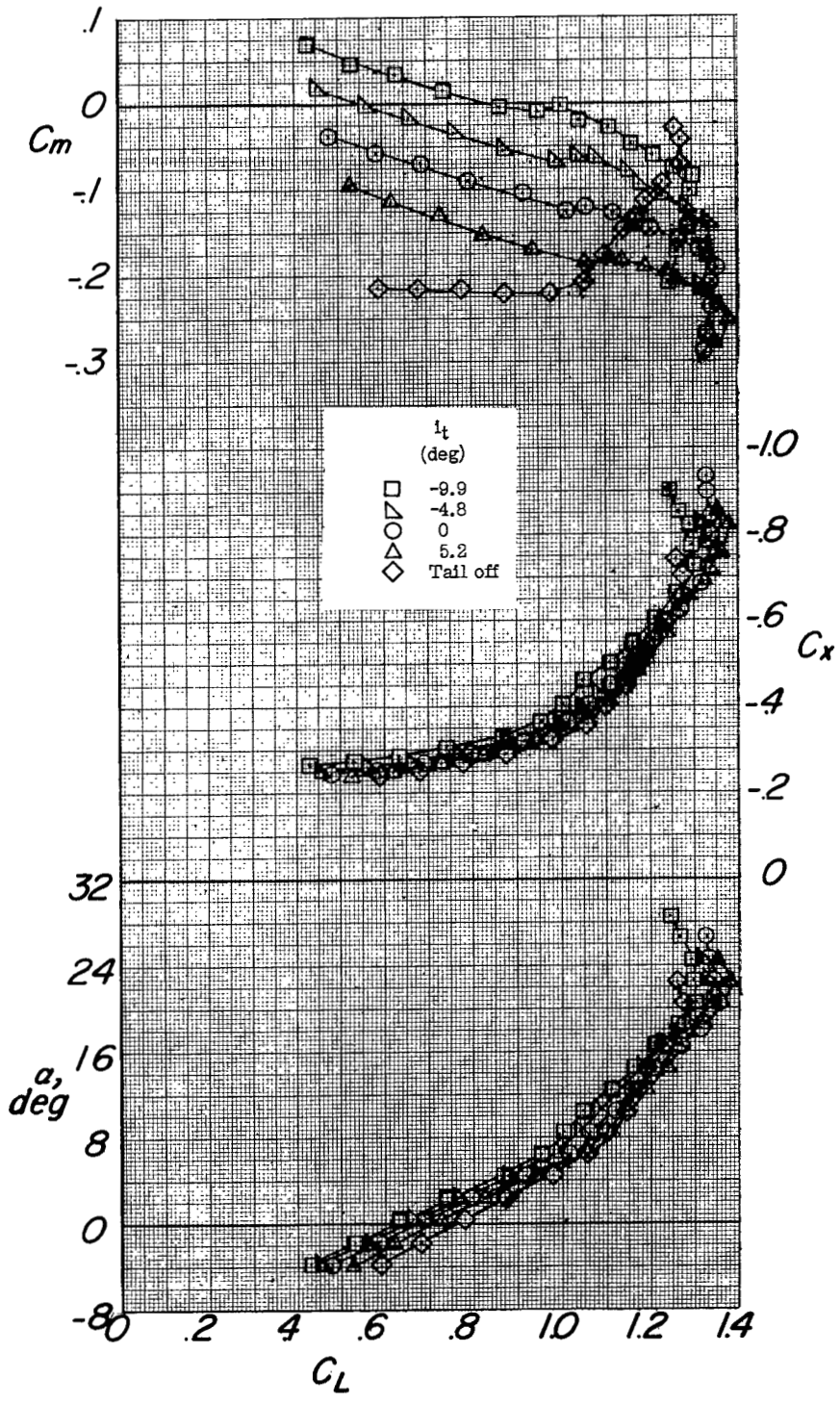

Figure 10.- The effect of the horizontal stabilizer on the aerodynamic characteristics in pitch. Configuration FWVH; $i_w = 0^\circ$; $\delta_f = 50^\circ$; brakes on; q = 49 lb/sq ft.

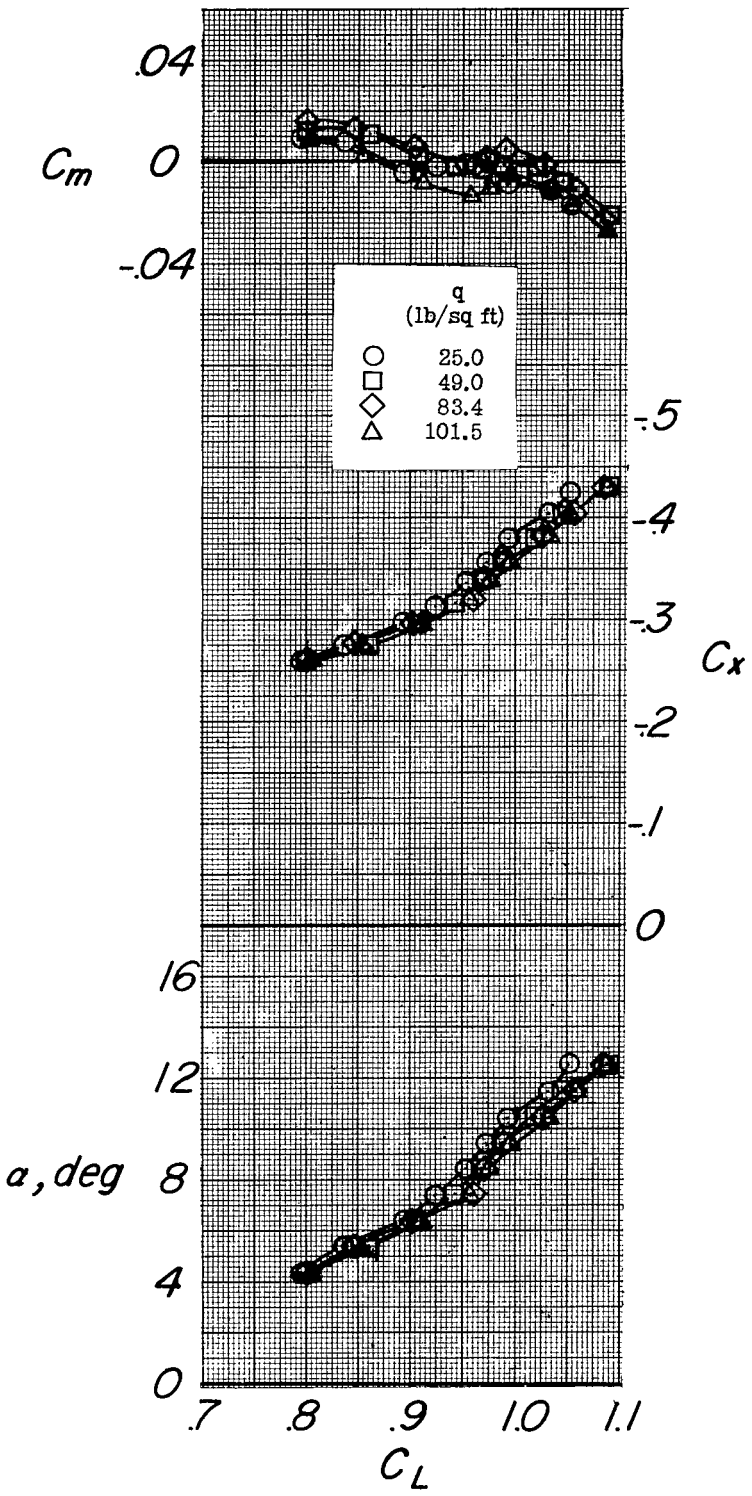

Figure 11.- The effect of dynamic pressure on the aerodynamic characteristics in pitch. Configuration FWVH; $i_w = 0^\circ$; $\delta_f = 43^\circ$; $i_t = -9.9^\circ$.

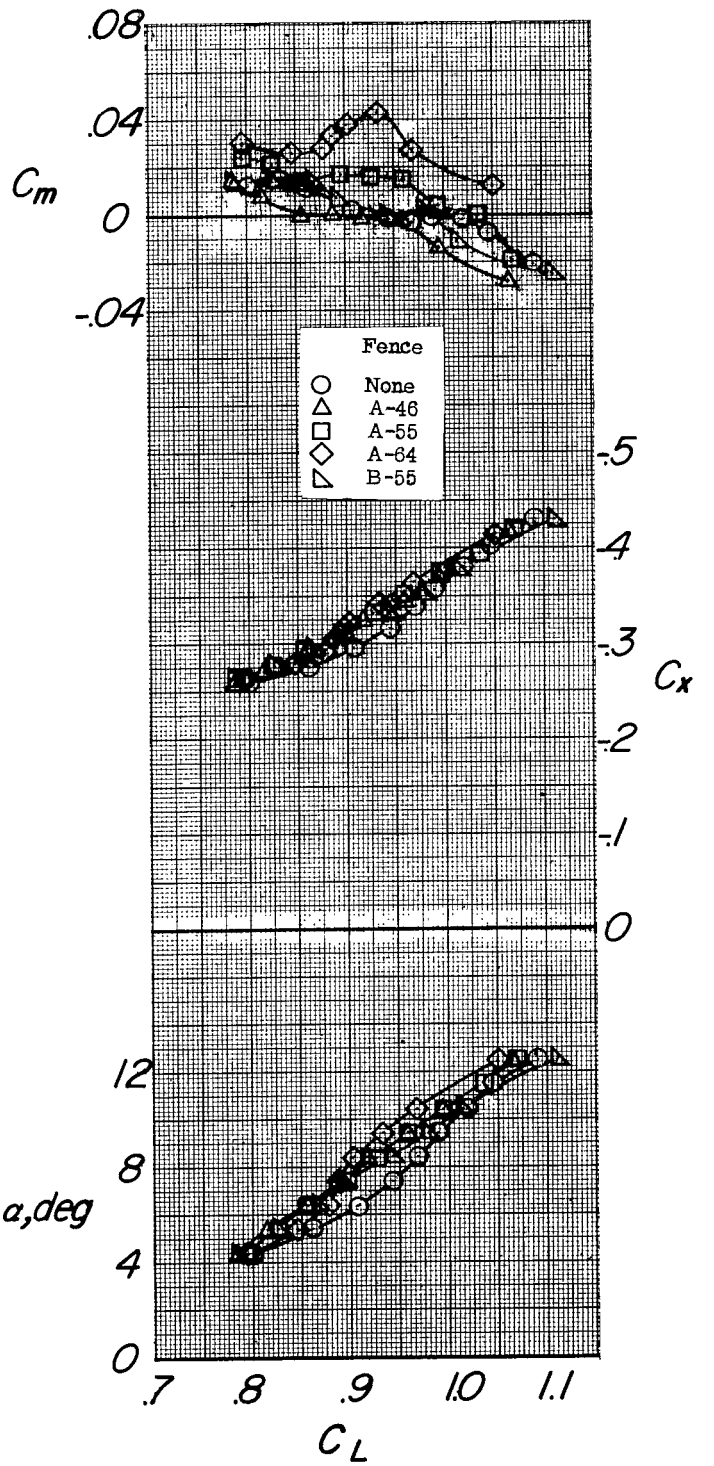

Figure 12.- The effect of flow fences on the aerodynamic characteristics in pitch. Configuration FWVH; $i_w = 0°$; $\delta_f = 43°$; $i_t = -9.9°$; $q = 49$ lb/sq ft.

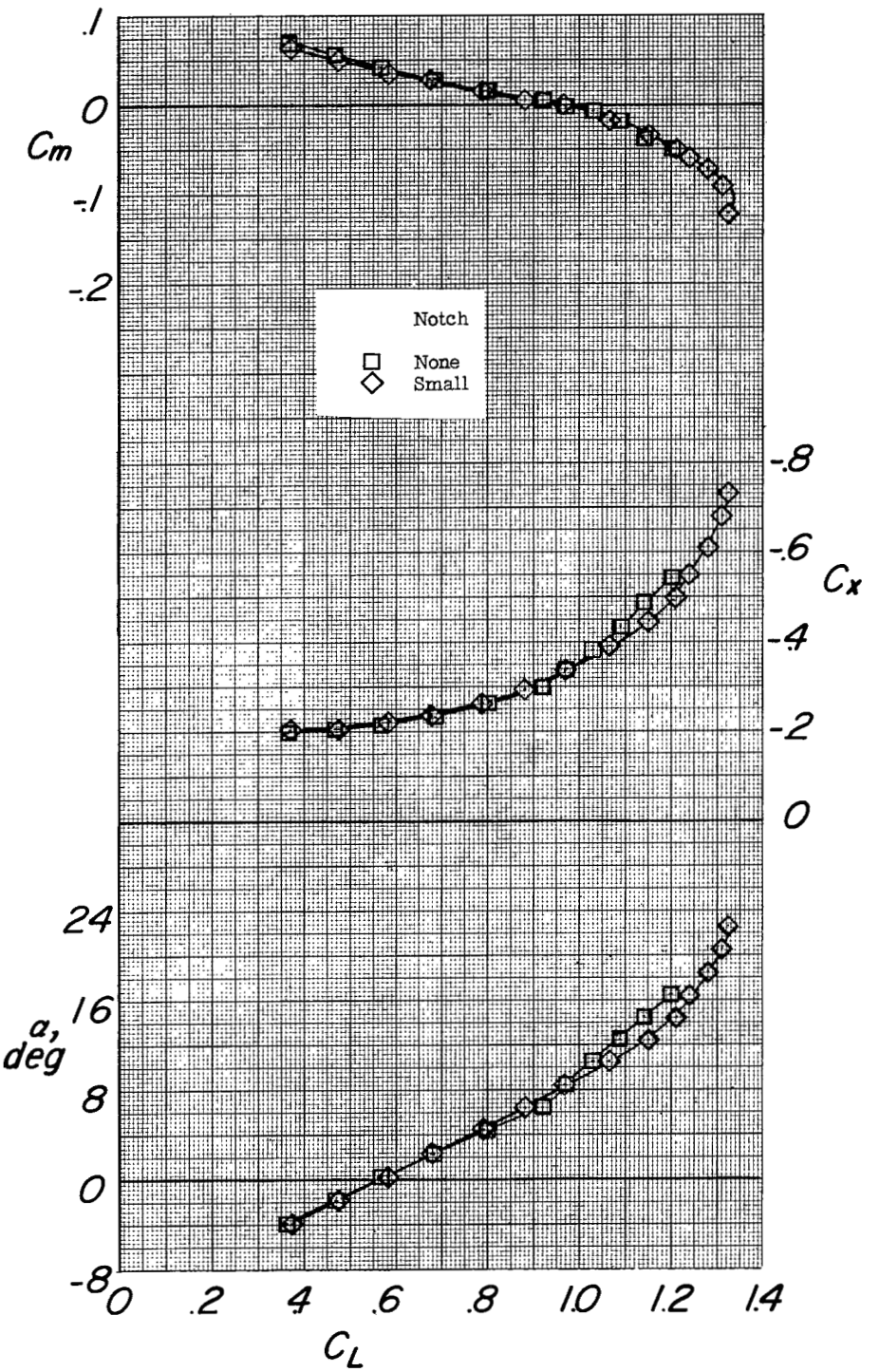

Figure 13.- The effect of leading-edge configuration on the aerodynamic characteristics in pitch. Configuration FWVH; $i_w = 0^\circ$; $\delta_f = 43^\circ$; $i_t = -9.9^\circ$; q = 83.4 lb/sq ft.

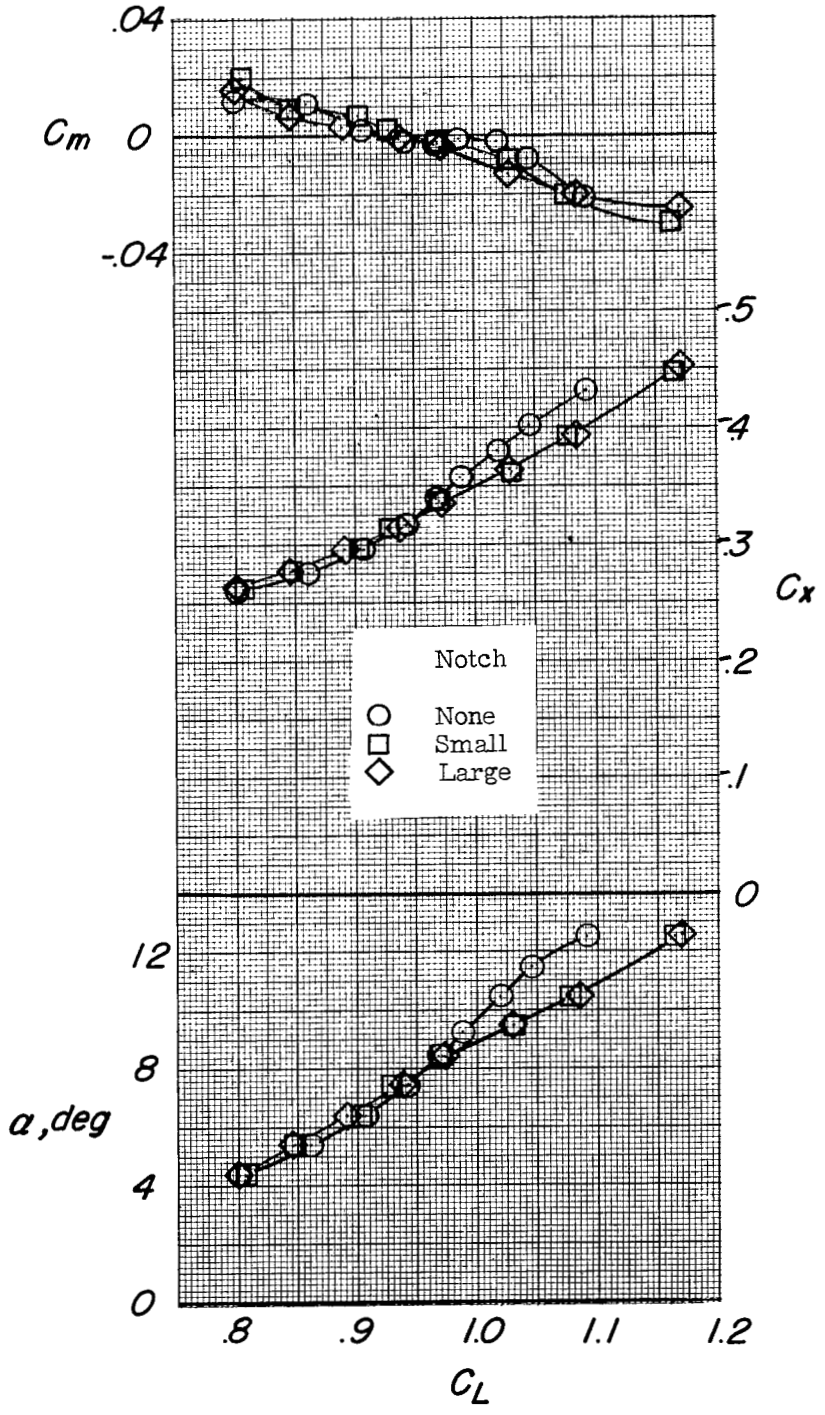

Figure 14.- The effect of leading-edge configuration on the aerodynamic characteristics in pitch. Configuration FWVH; $i_w = 0^\circ$; $\delta_f = 43^\circ$; $i_t = -9.9^\circ$; q = 49 lb/sq ft.

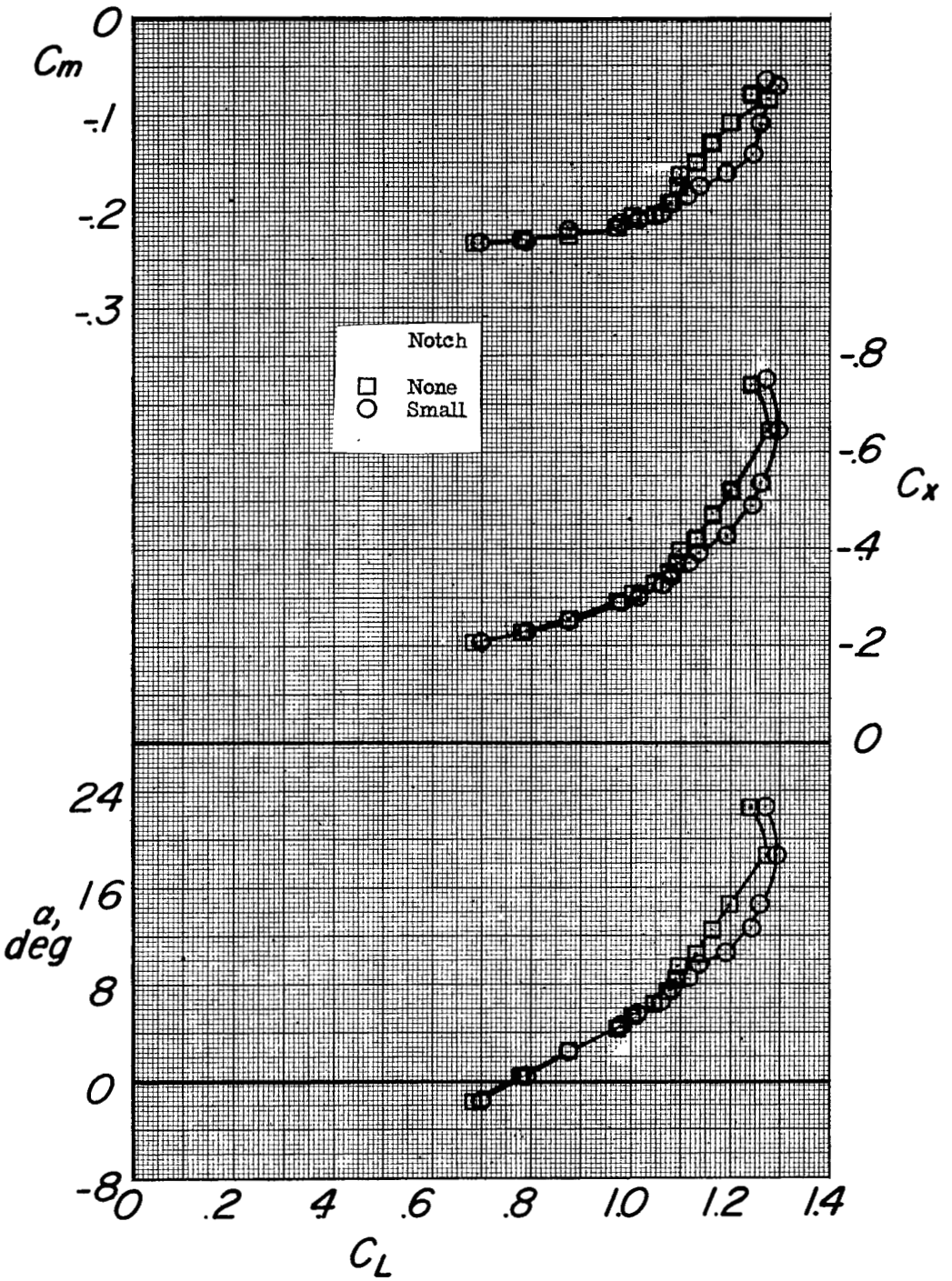

(a) Tail off; configuration FWV.

Figure 15.- The effect of leading-edge configuration on the aerodynamic characteristics in pitch. $i_w = 0^\circ$; $\delta_f = 50^\circ$; q = 49 lb/sq ft.

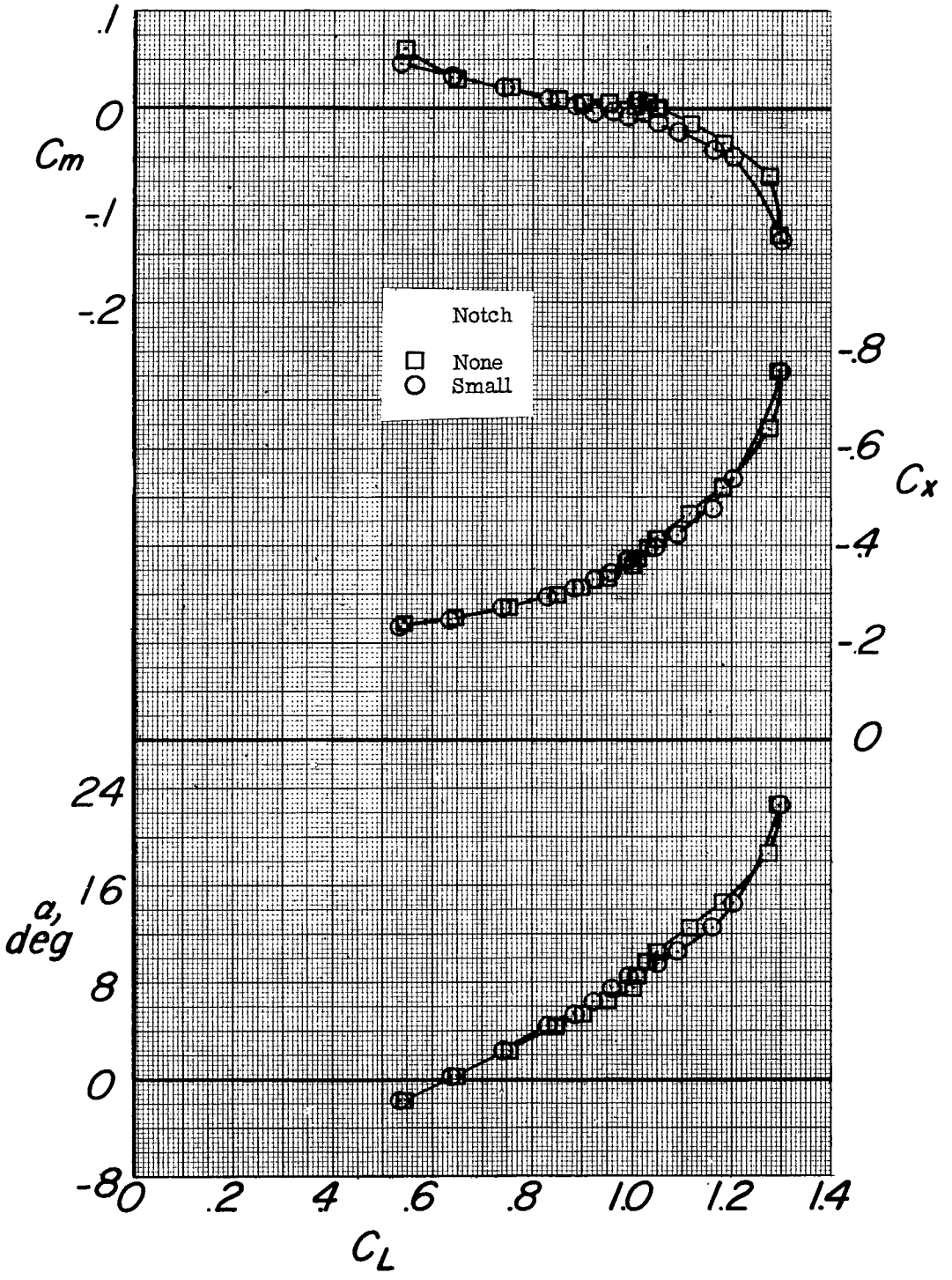

(b) $i_t = -9.9^\circ$; configuration FWVH.

Figure 15.- Concluded.

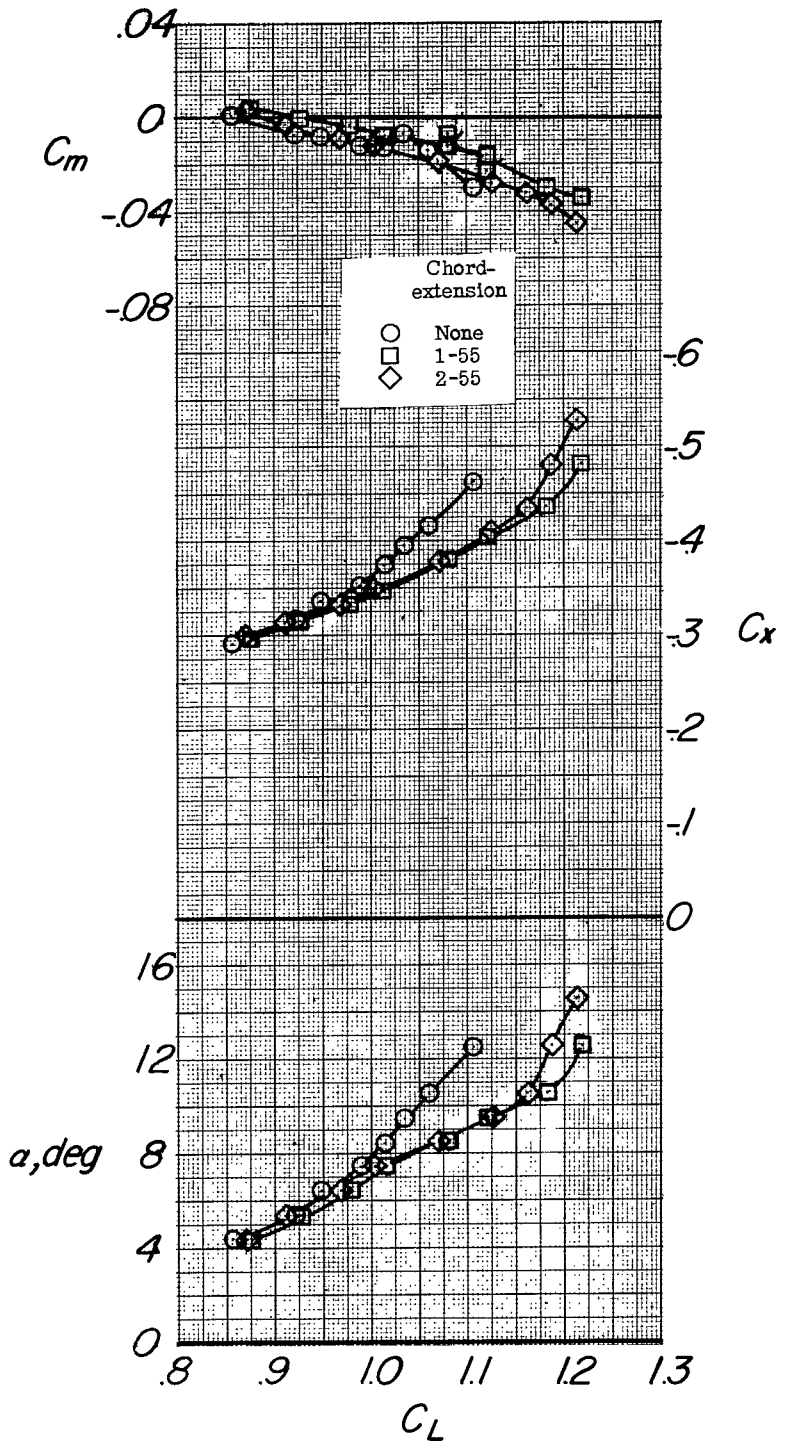

Figure 16.- The effect of leading-edge extensions on the aerodynamic characteristics in pitch. Configuration FWVH; $i_w = 0^\circ$; $\delta_f = 50^\circ$; $i_t = -9.9^\circ$; q = 49 lb/sq ft.

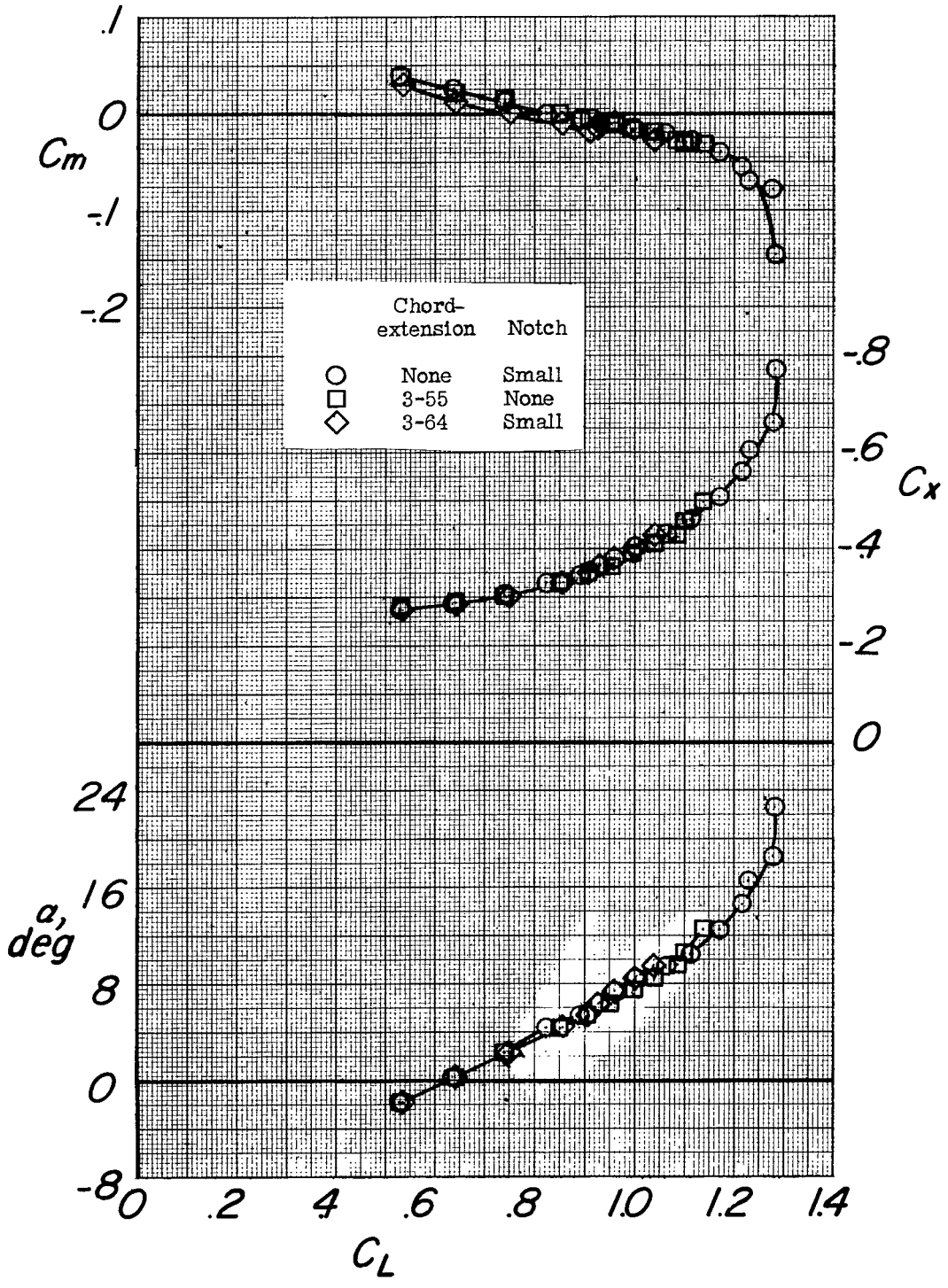

Figure 17.- The effect of leading-edge configuration on the aerodynamic characteristics in pitch. Configuration FWVH; $i_w = 0^\circ$; $\delta_f = 50^\circ$; $i_t = -9.9^\circ$; brakes on; q = 49 lb/sq ft.

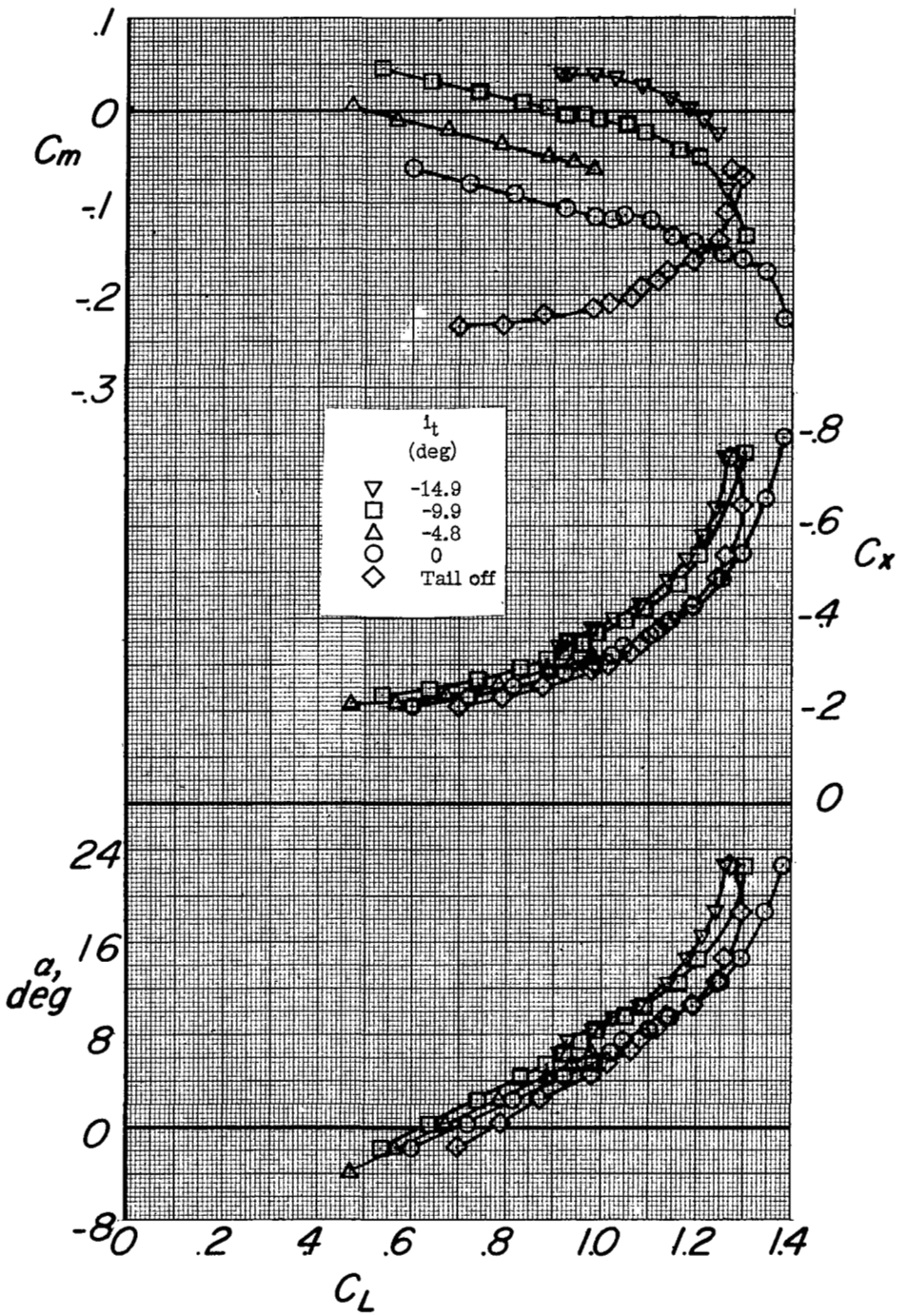

(a) Tanks off; brakes off.

Figure 18.- The effect of the horizontal stabilizer on the aerodynamic characteristics in pitch. Configuration FWVH; $i_w = 0^\circ$; $\delta_f = 50^\circ$; small notch; q = 49 lb/sq ft.

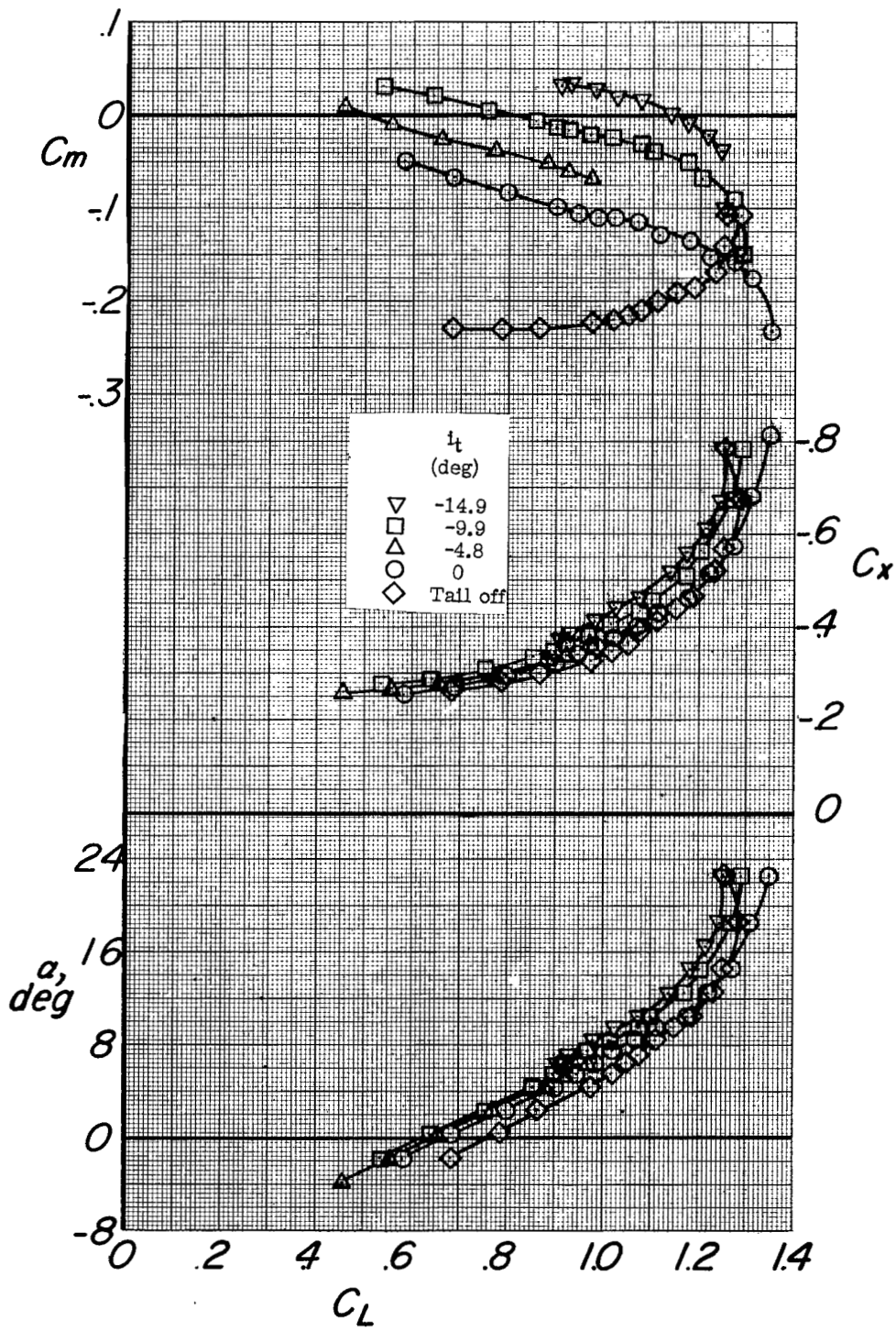

(b) Tanks off; brakes on.

Figure 18.- Continued.

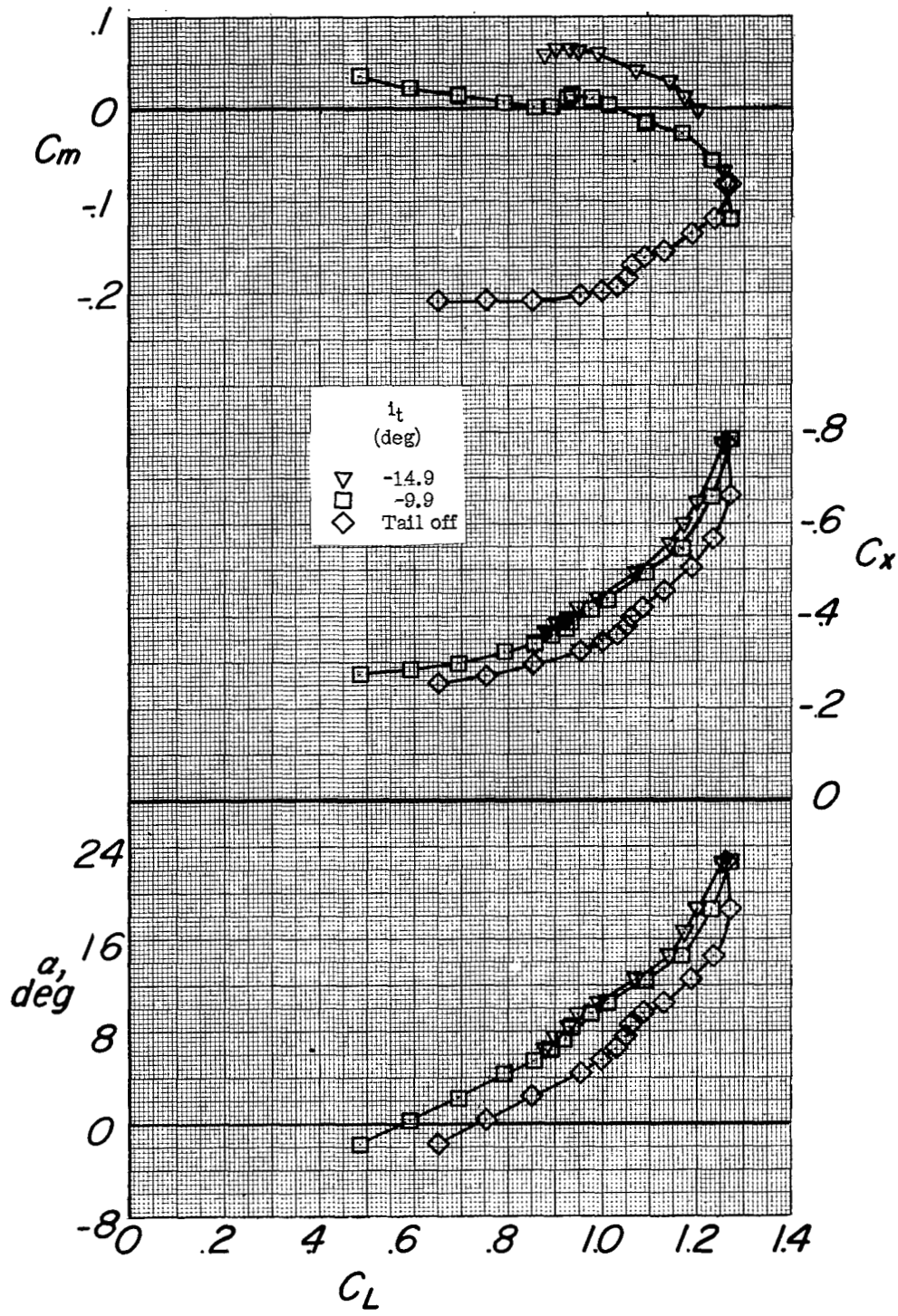

(c) Tanks and pylons on at 0.33b/2; brakes on.

Figure 18.- Concluded.

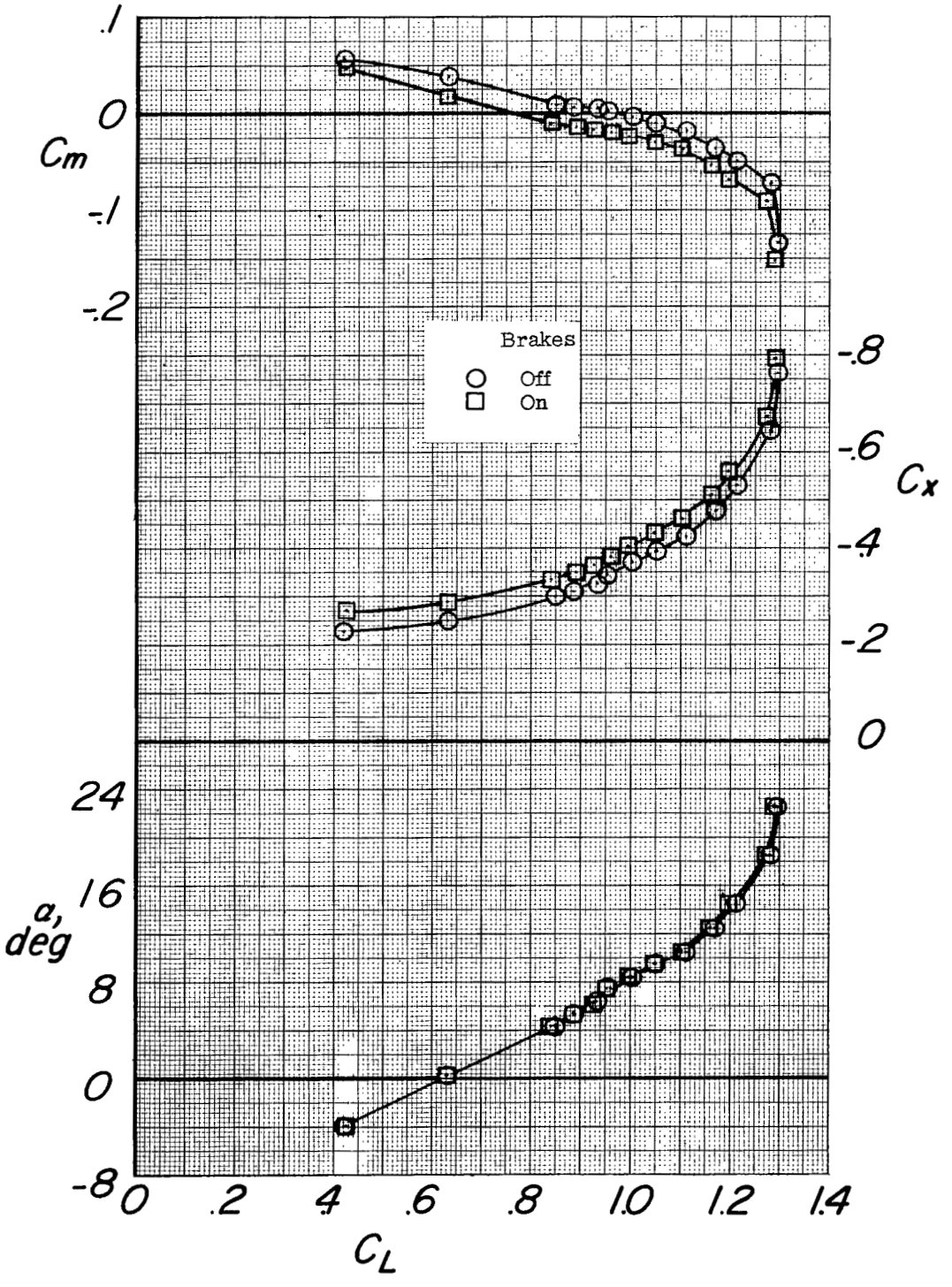

Figure 19.- The effect of brakes on the aerodynamic characteristics in pitch. Configuration FWVH; $i_w = 0^\circ$; $\delta_f = 50^\circ$; $i_t = -9.9^\circ$; small notch; q = 49 lb/sq ft.

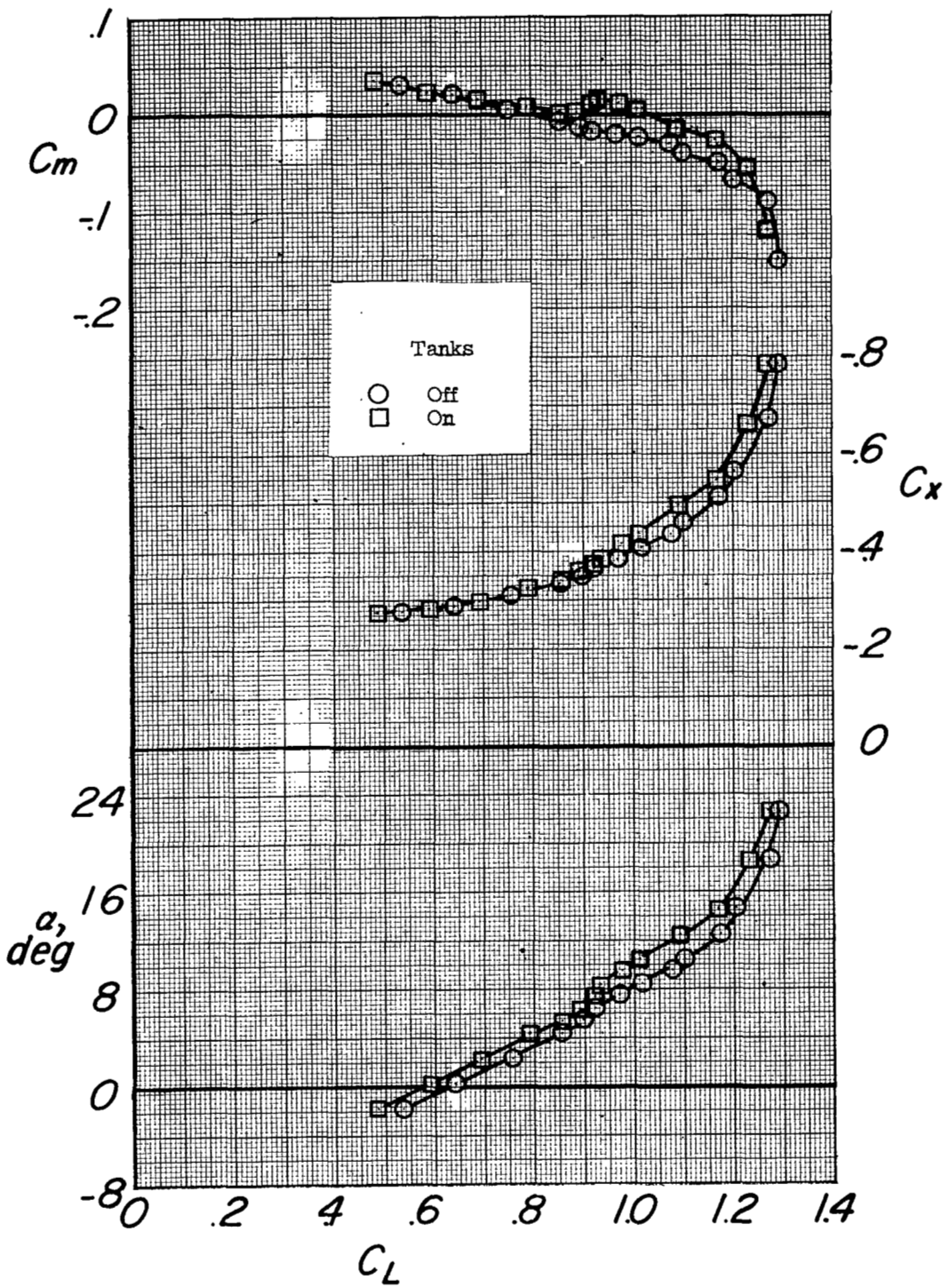

Figure 20.- The effect of tanks on the aerodynamic characteristics in pitch. Configuration FWVH; $i_w = 0^\circ$; $\delta_f = 50^\circ$; $i_t = -9.9^\circ$; small notch; brakes on; q = 49 lb/sq ft.

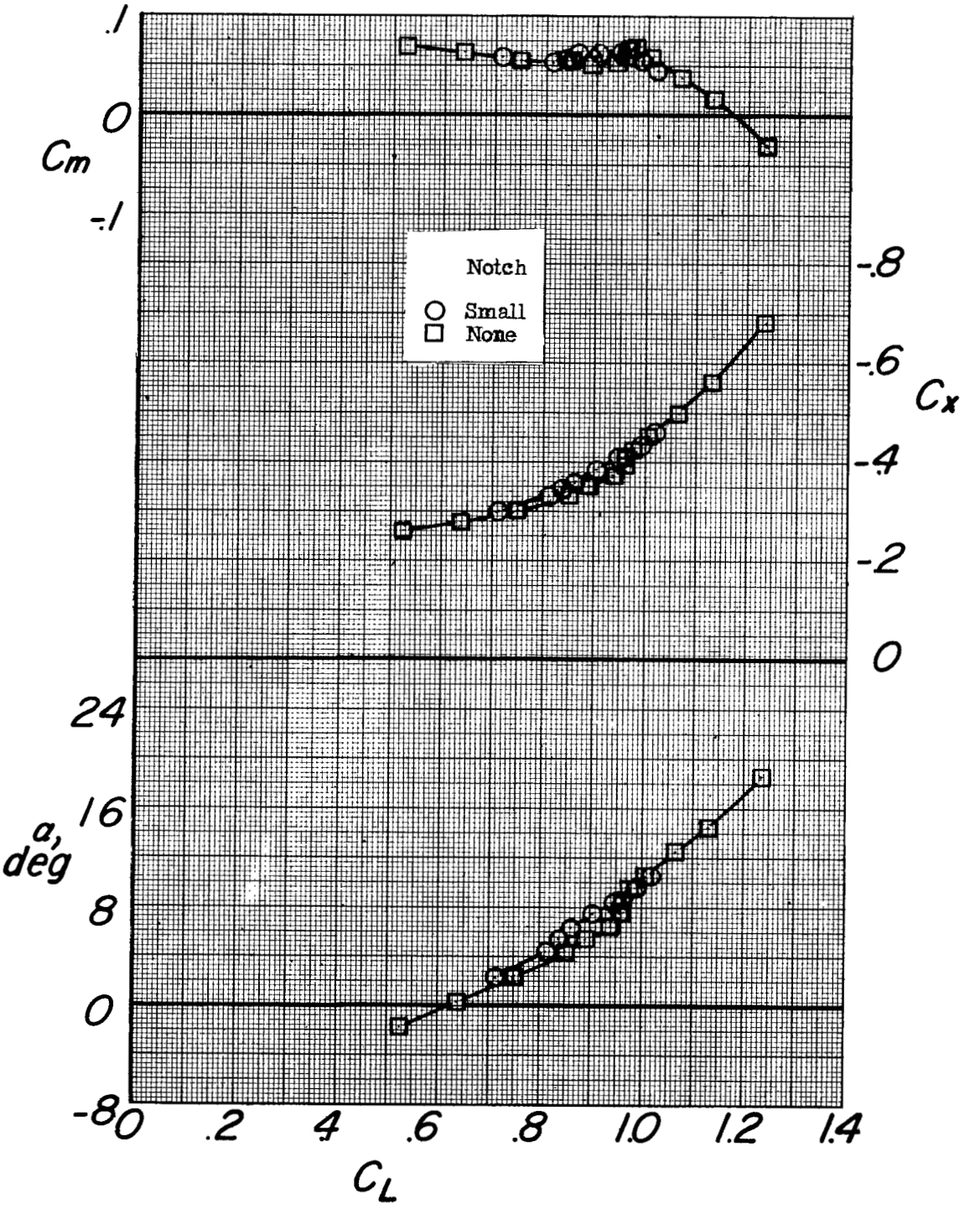

Figure 21.- The effect of leading-edge configuration on the aerodynamic characteristics in pitch. Configuration FWVH; $i_w = 2^\circ$; $\delta_f = 43^\circ$; $i_t = -9.9^\circ$; tanks on; brakes on; q = 49 lb/sq ft.

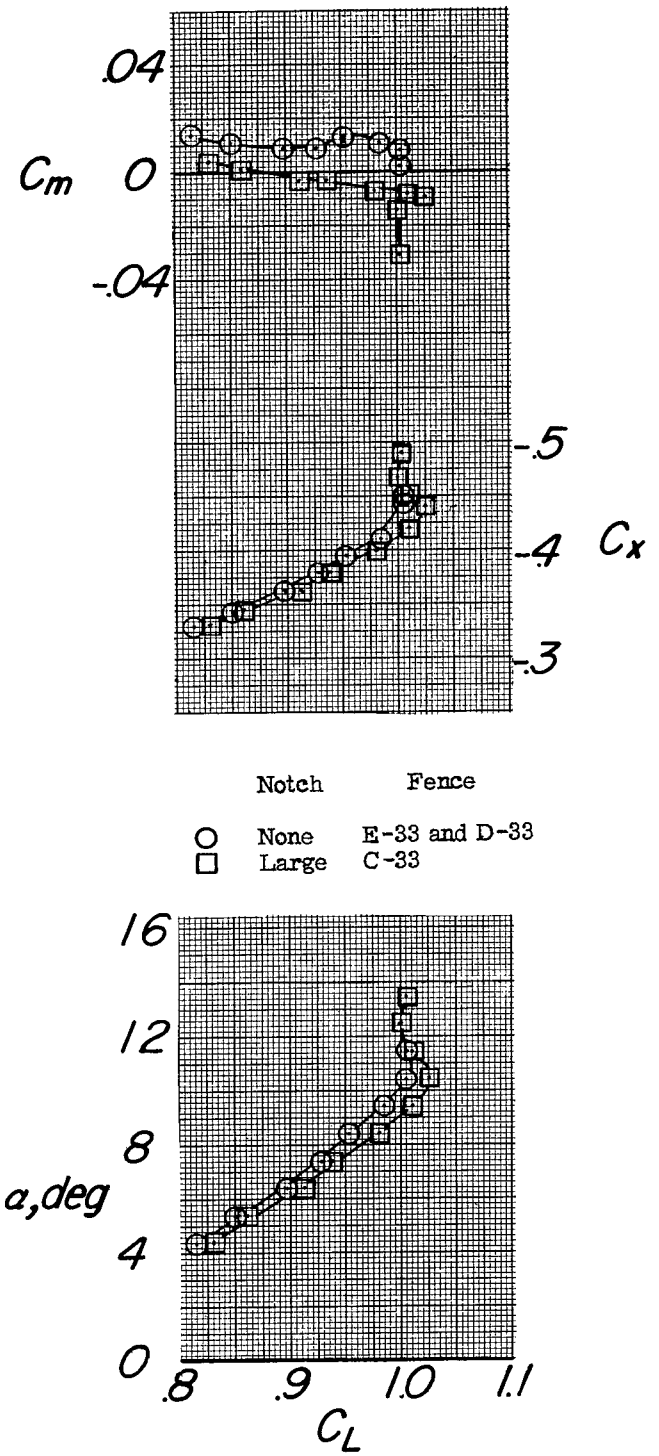

Figure 22.- The aerodynamic characteristics in pitch of two fence and notch configurations. Configuration FWVH; $i_w = 0^\circ$; $\delta_f = 50^\circ$; $i_t = -9.9^\circ$; brakes on; pylons on lower surface of wing without tanks at 0.33b/2; q = 49 lb/sq ft.

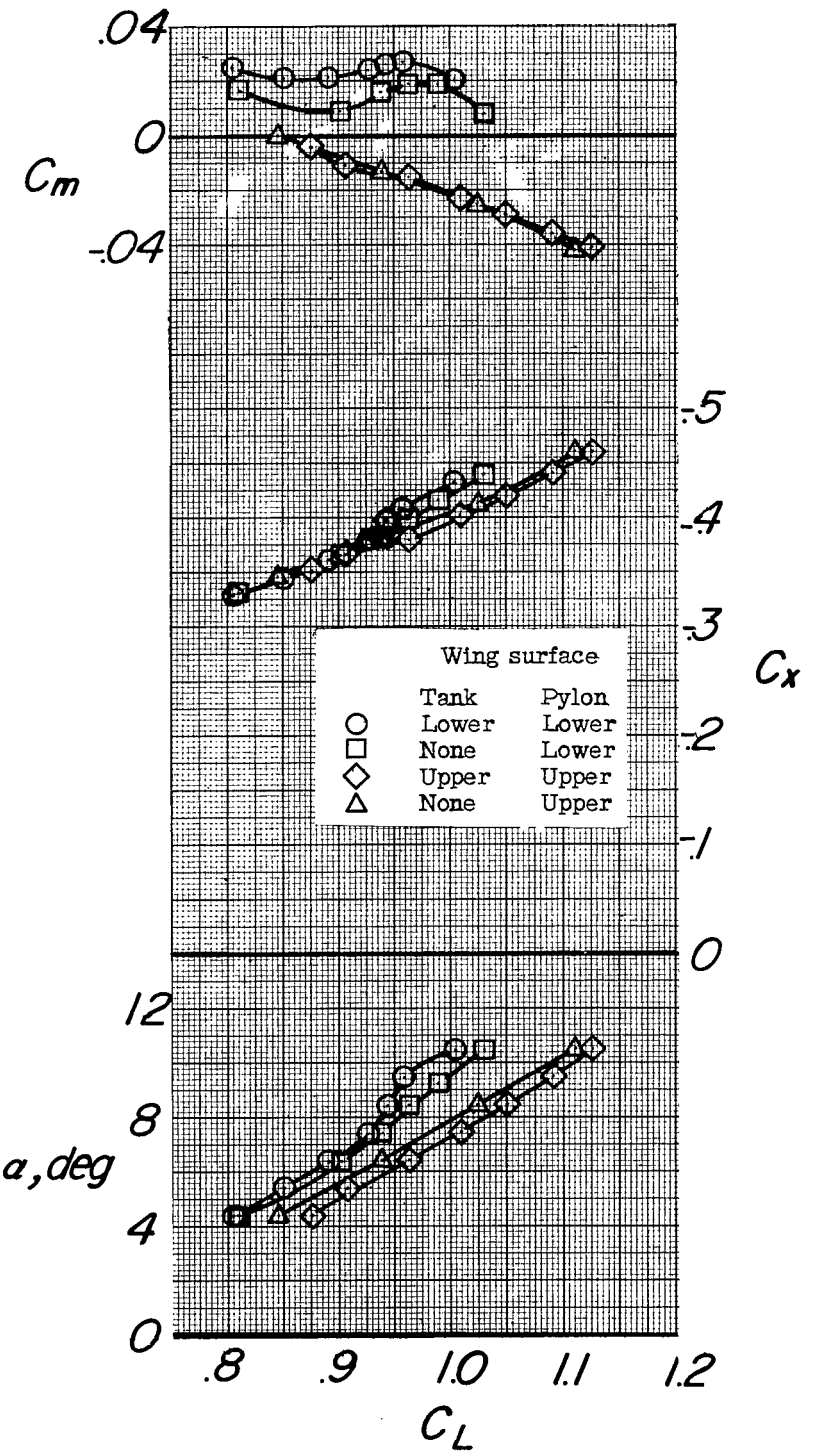

Figure 23.- The effect of tank and pylon configuration on the aerodynamic characteristics in pitch. Configuration FWVH; $i_w = 0^\circ$; $\delta_f = 50^\circ$; $i_t = -9.9^\circ$; fence E-55; brakes on; q = 49 lb/sq ft.

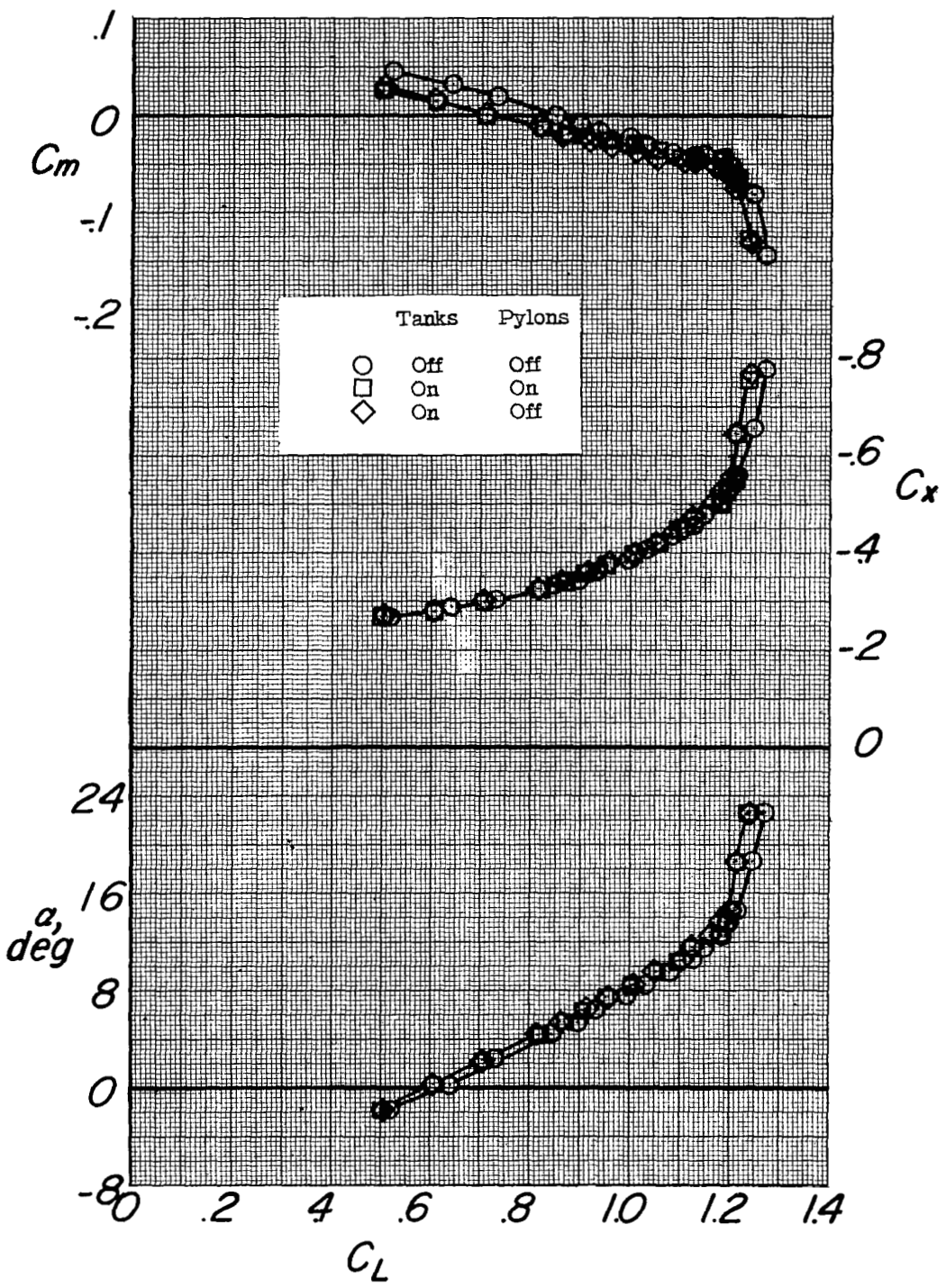

Figure 24.- The effect of tanks and pylons on the aerodynamic characteristics in pitch (tanks and pylons located at 0.184b/2). Configuration FWVH; $i_w = 0^\circ$; $\delta_f = 50^\circ$; $i_t = -9.9^\circ$; fence E-33; small notch; brakes on; q = 49 lb/sq ft.

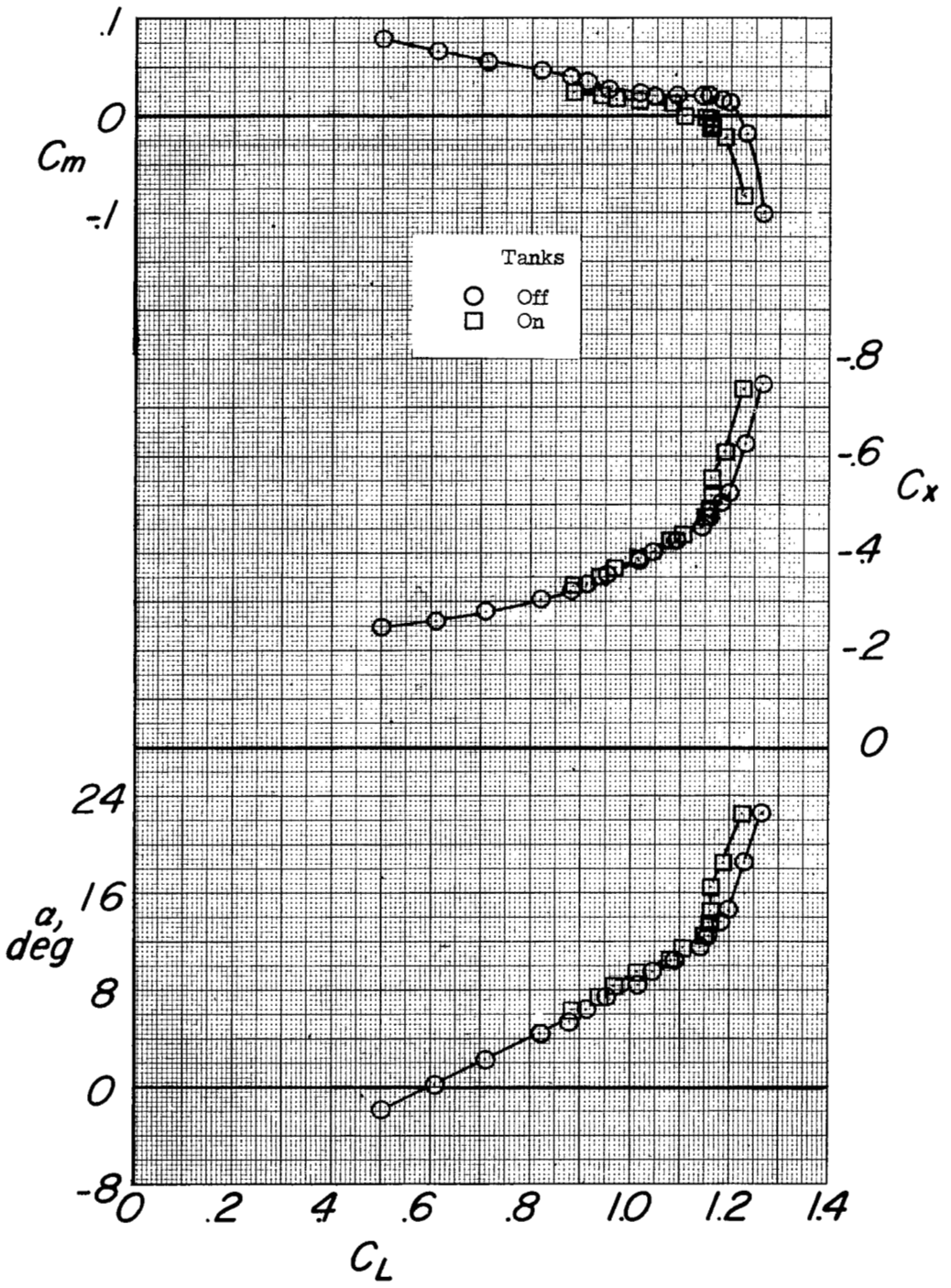

Figure 25.- The effect of the tanks on the aerodynamic characteristics in pitch. Configuration FWVH; $i_w = 0^\circ$; $\delta_f = 50^\circ$; $i_t = -14.9^\circ$; small notch; upper main-landing-gear doors on; fence E-33; tank location, 0.184b/2; q = 49 lb/sq ft.

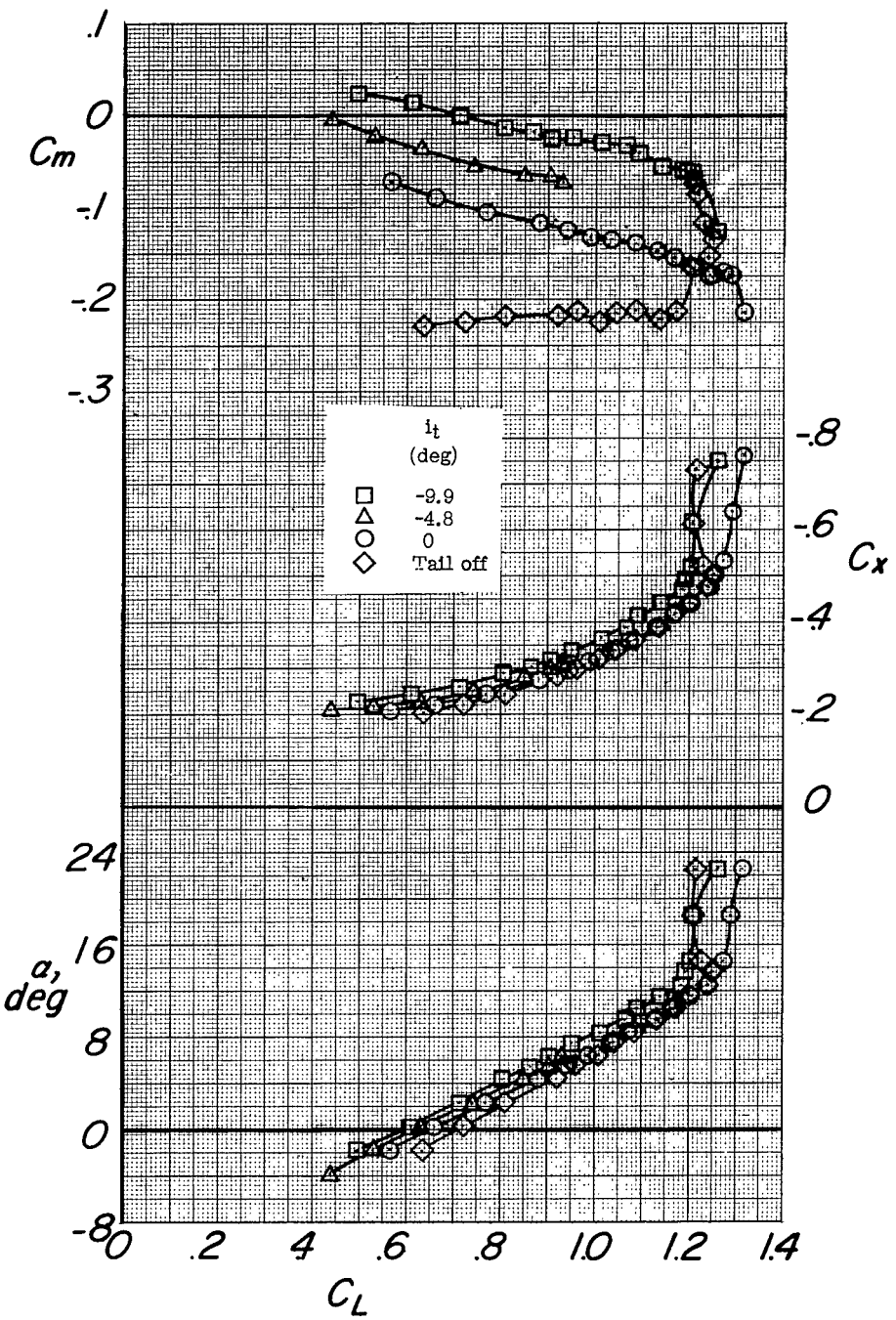

(a) Brakes off.

Figure 26.- The effect of the horizontal stabilizer on the aerodynamic characteristics in pitch. Configuration FWVH; $i_w = 0^\circ$; $\delta_f = 50^\circ$; tanks-184; small notch; fence E-33; q = 49 lb/sq ft; top main-landing-gear doors on.

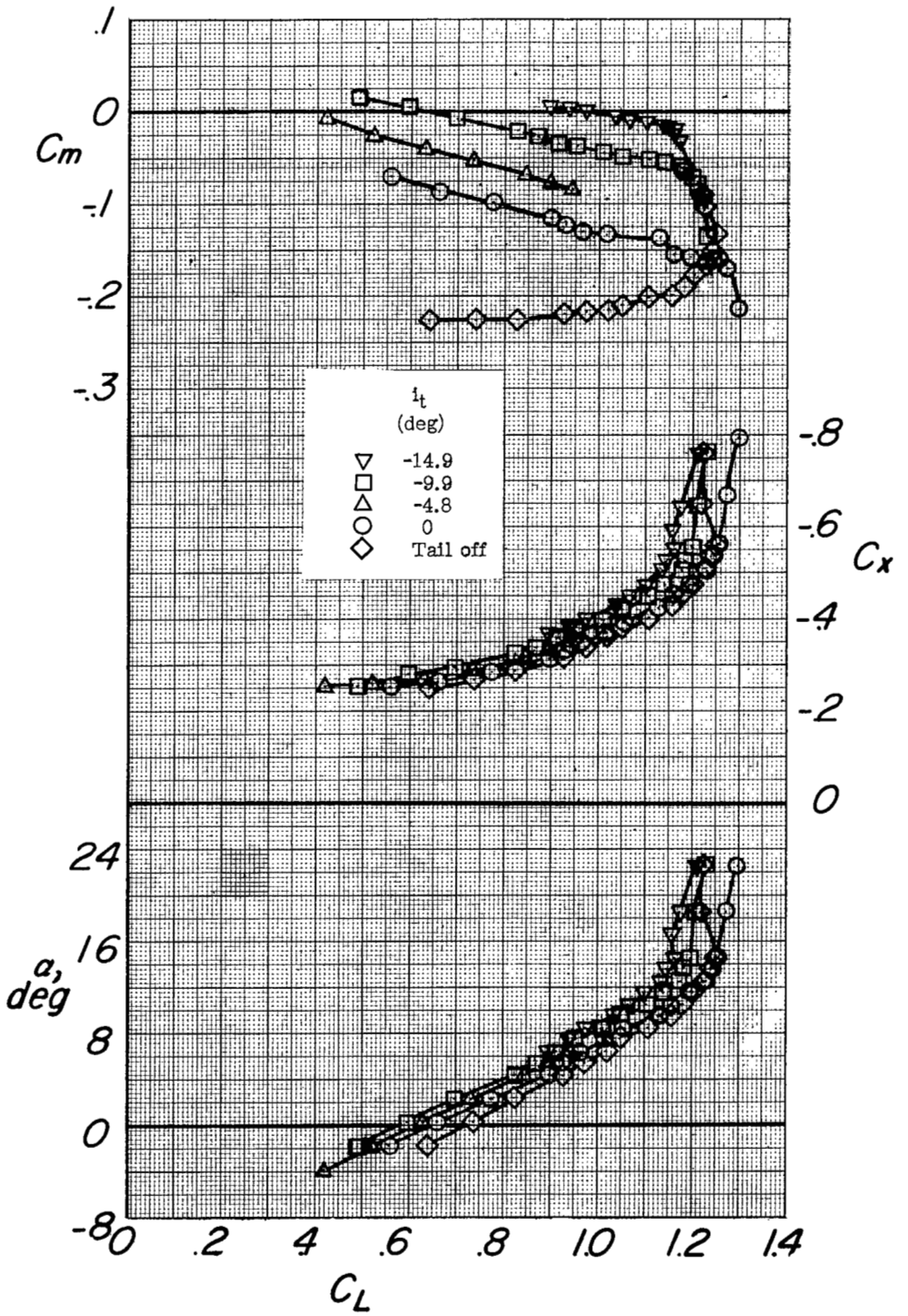

(b) Brakes on.

Figure 26.- Concluded.

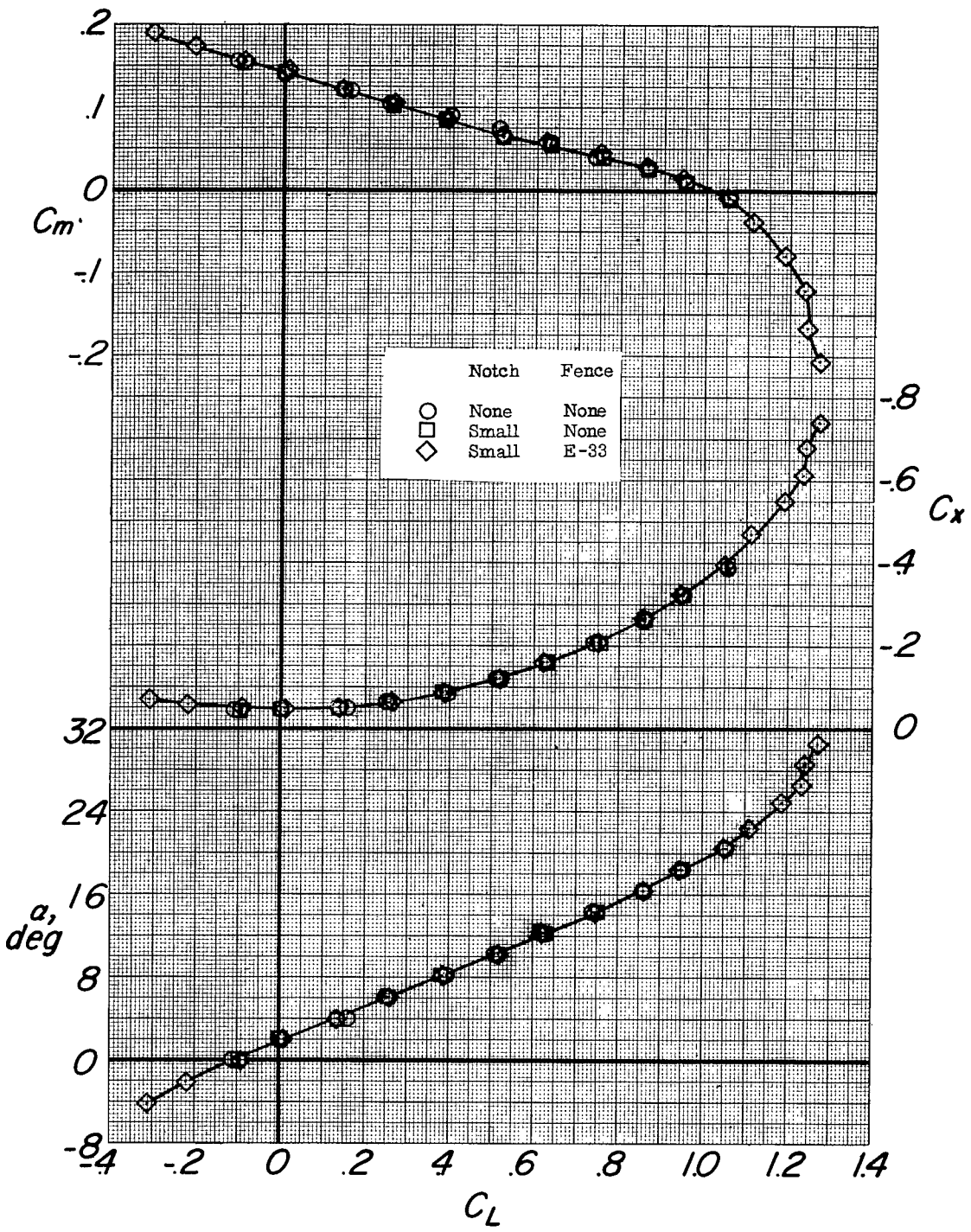

(a) $i_t = -9.9^\circ$; configuration FWVH.

Figure 27.- The effect of leading-edge configuration on the aerodynamic characteristics in pitch. $i_w = 0^\circ$; $\delta_f = 0^\circ$; q = 49 lb/sq ft.

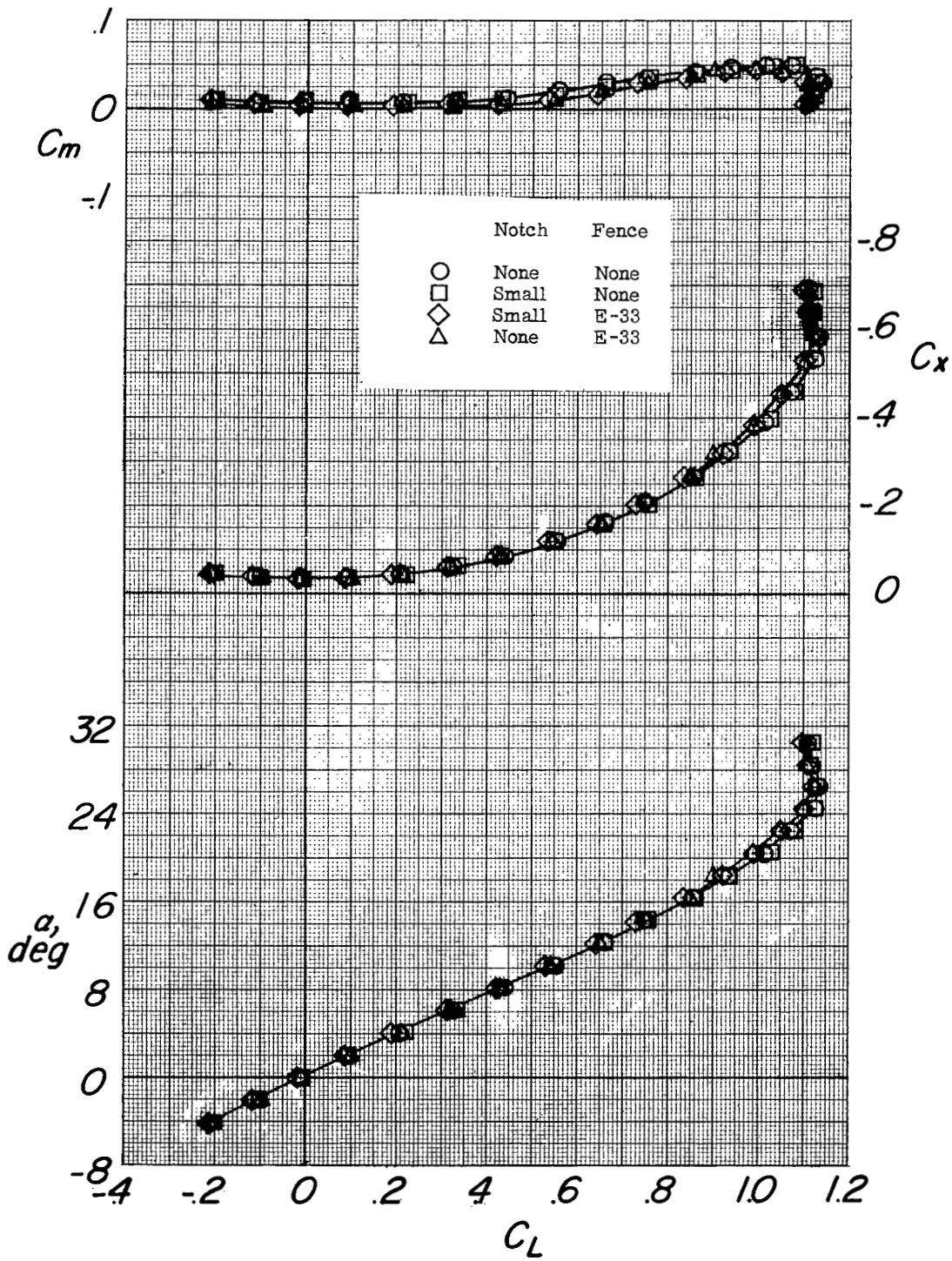

(b) Horizontal tail off; configuration FWV.

Figure 27.- Concluded.

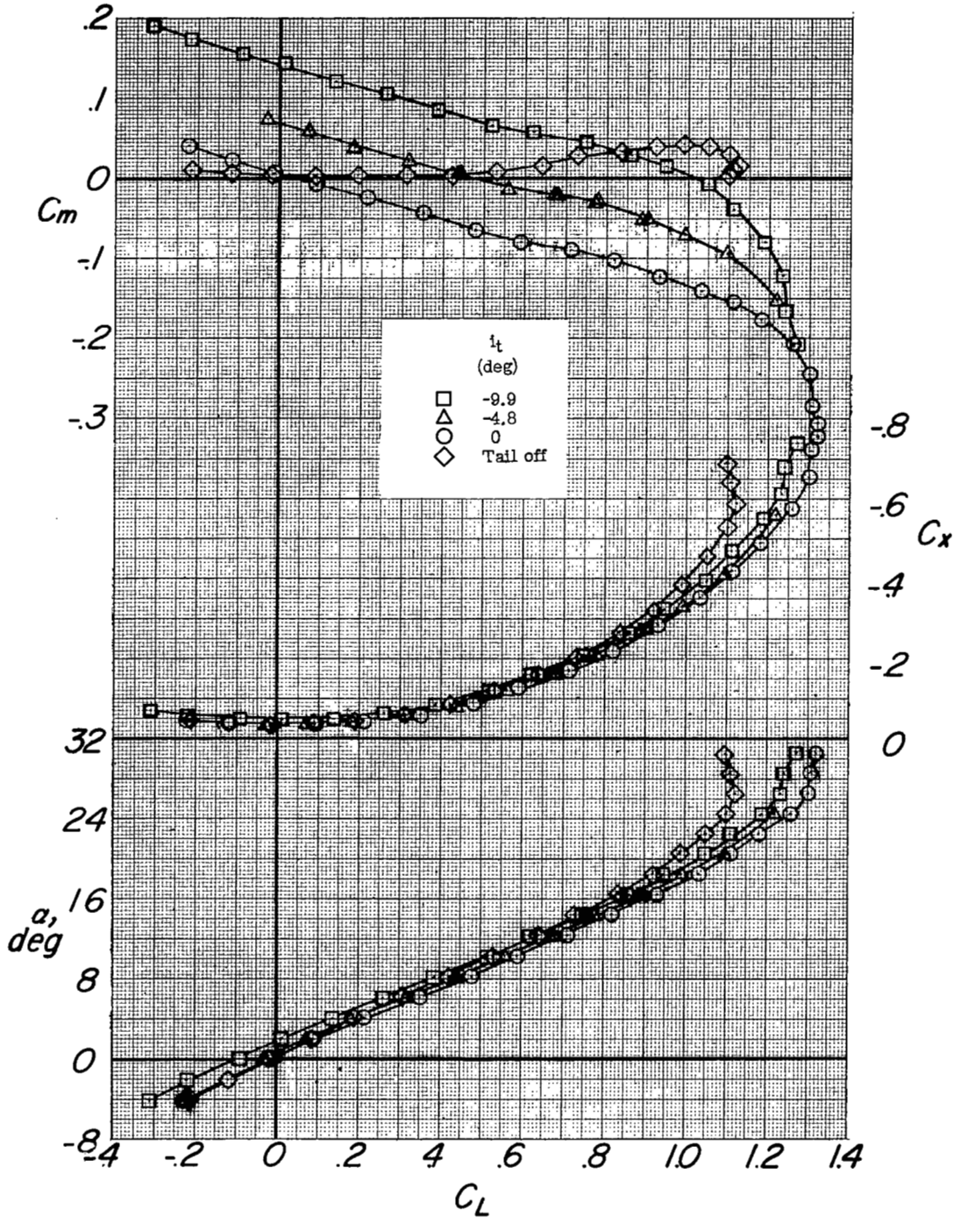

(a) Tanks off; brakes off.

Figure 28.- The effect of the horizontal stabilizer on the aerodynamic characteristics in pitch. Configuration FWVH; $i_w = 0^o$; $\delta_f = 0^o$; small notch; fence E-33; q = 49 lb/sq ft.

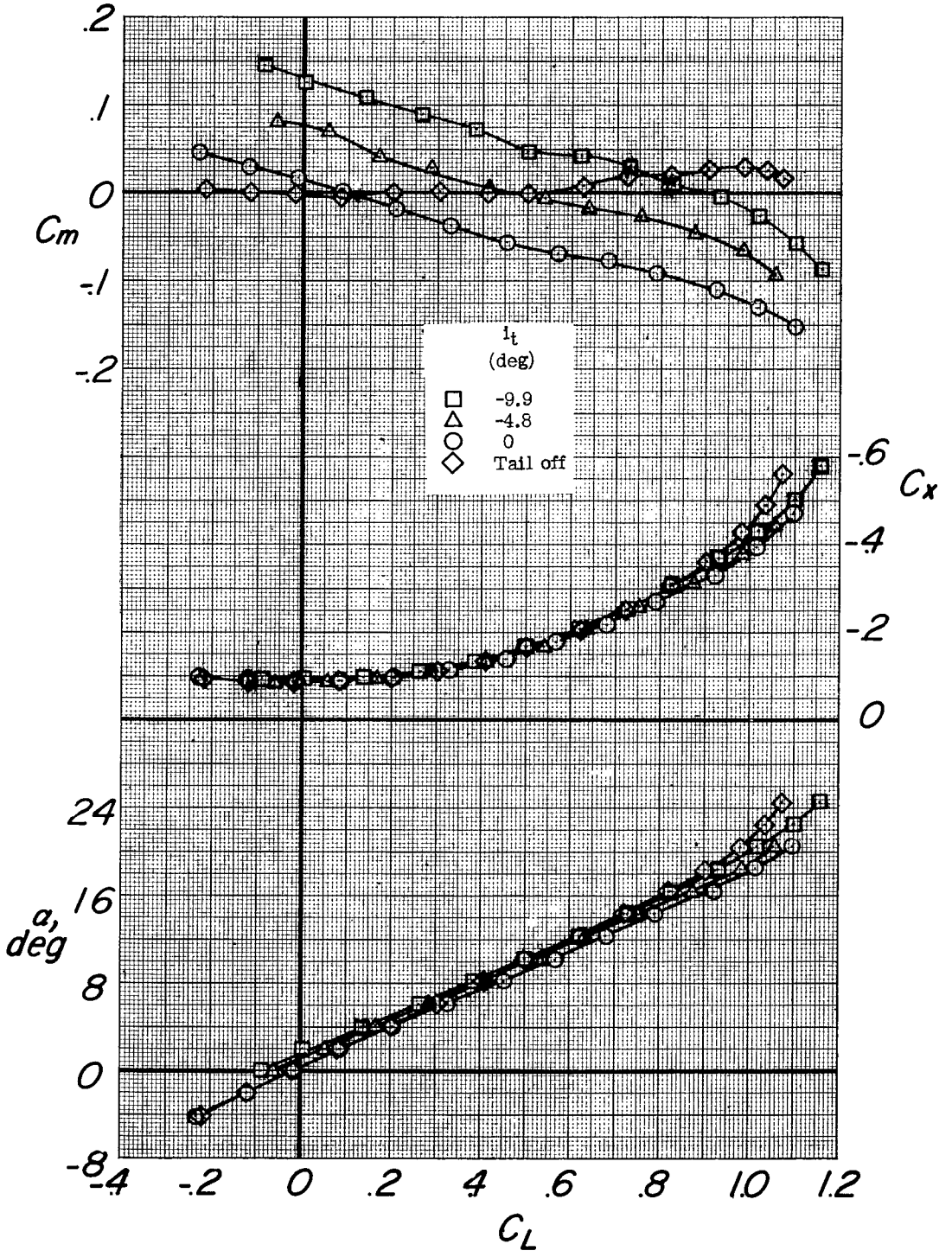

(b) Tanks off; brakes on.

Figure 28.- Continued.

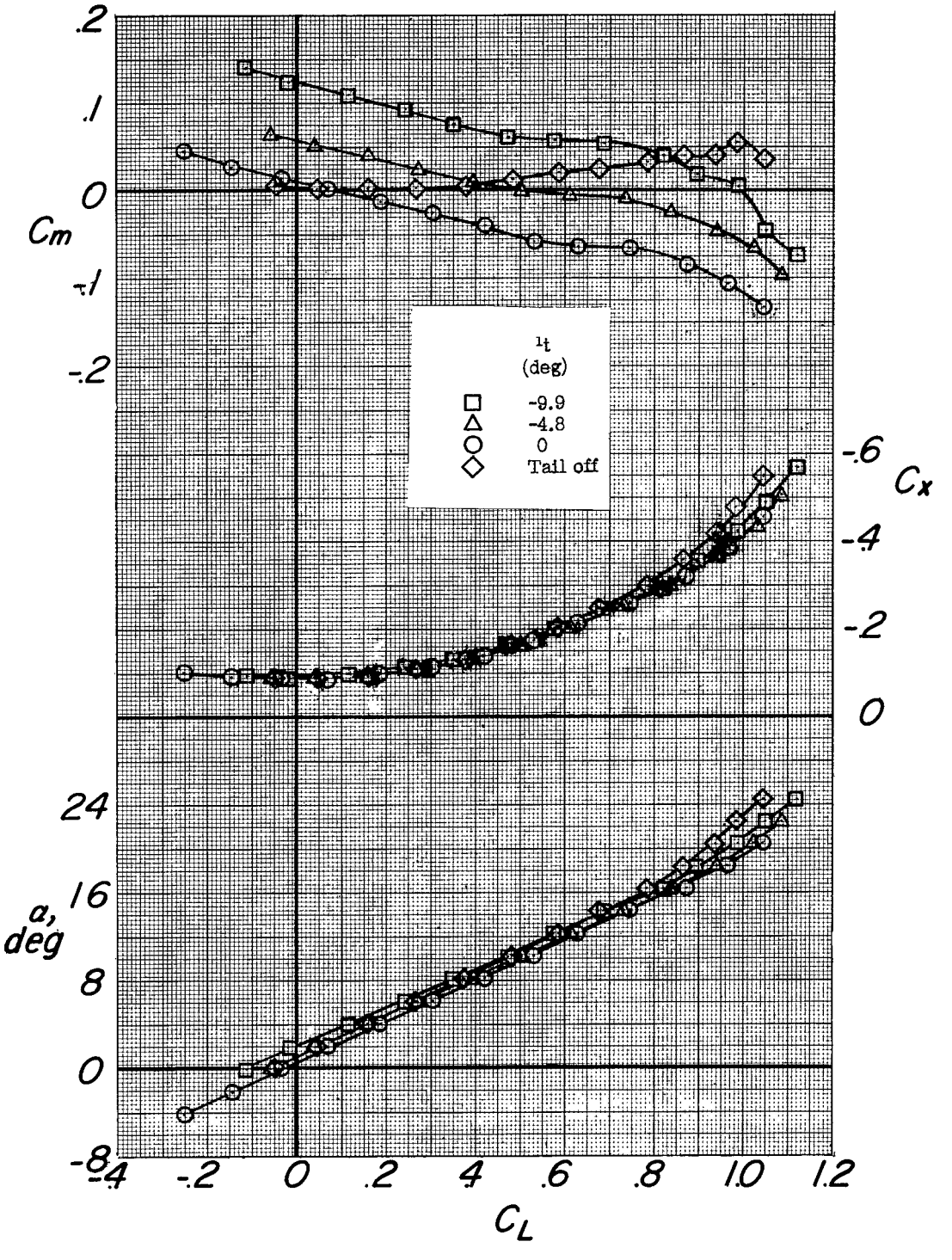

(c) Tanks and pylons on at 0.184b/2; brakes on.

Figure 28.- Continued.

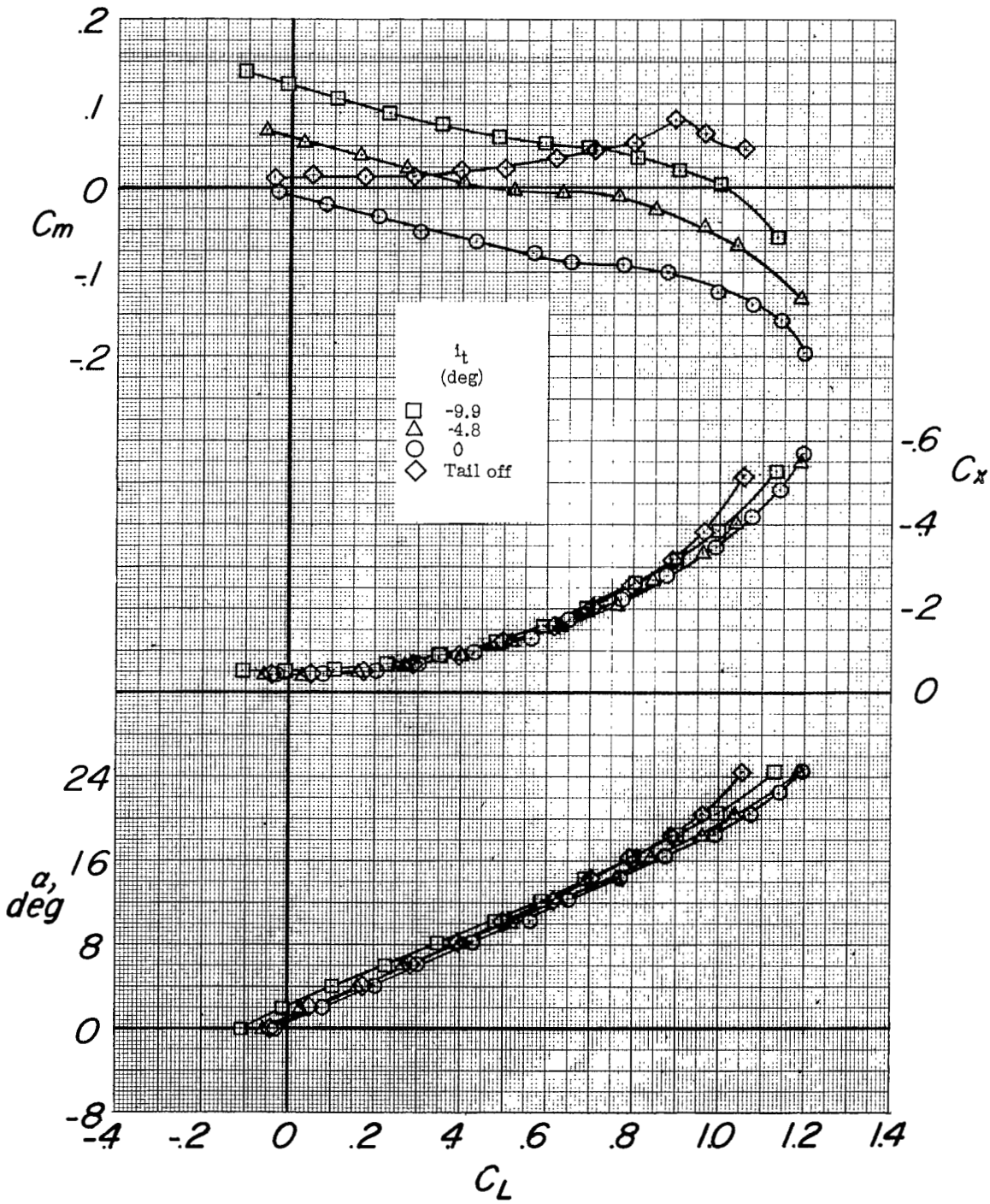

(d) Tanks and pylons on at 0.184b/2; brakes off.

Figure 28.- Concluded.

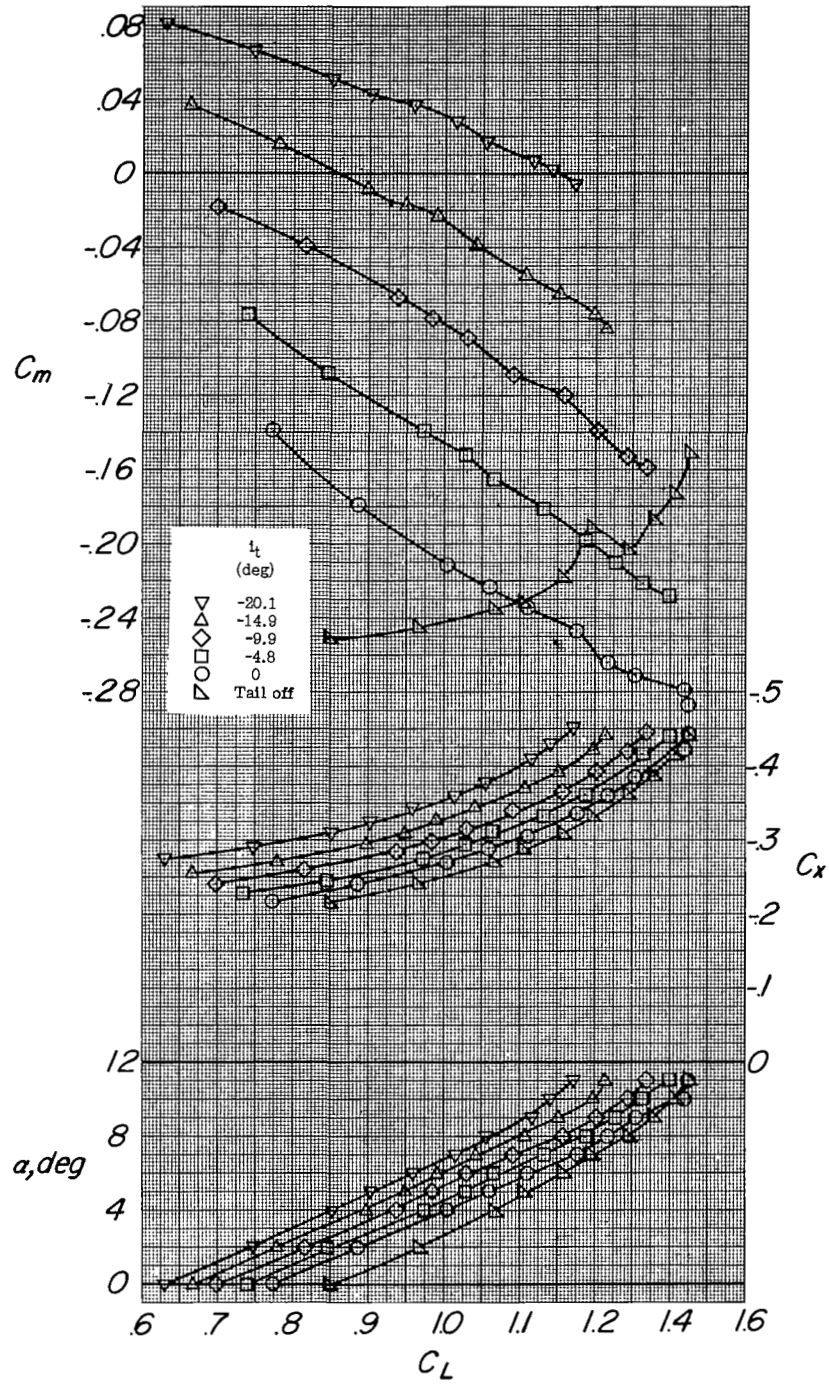

(a) Tanks off; brakes off.

Figure 29.- The effect of the horizontal stabilizer on the aerodynamic characteristics in pitch. Configuration FWVH; $i_w = 0^\circ$; $\delta_f = 50^\circ$; small notch; ground board H = 12.5 in.; q = 52.5 lb/sq ft.

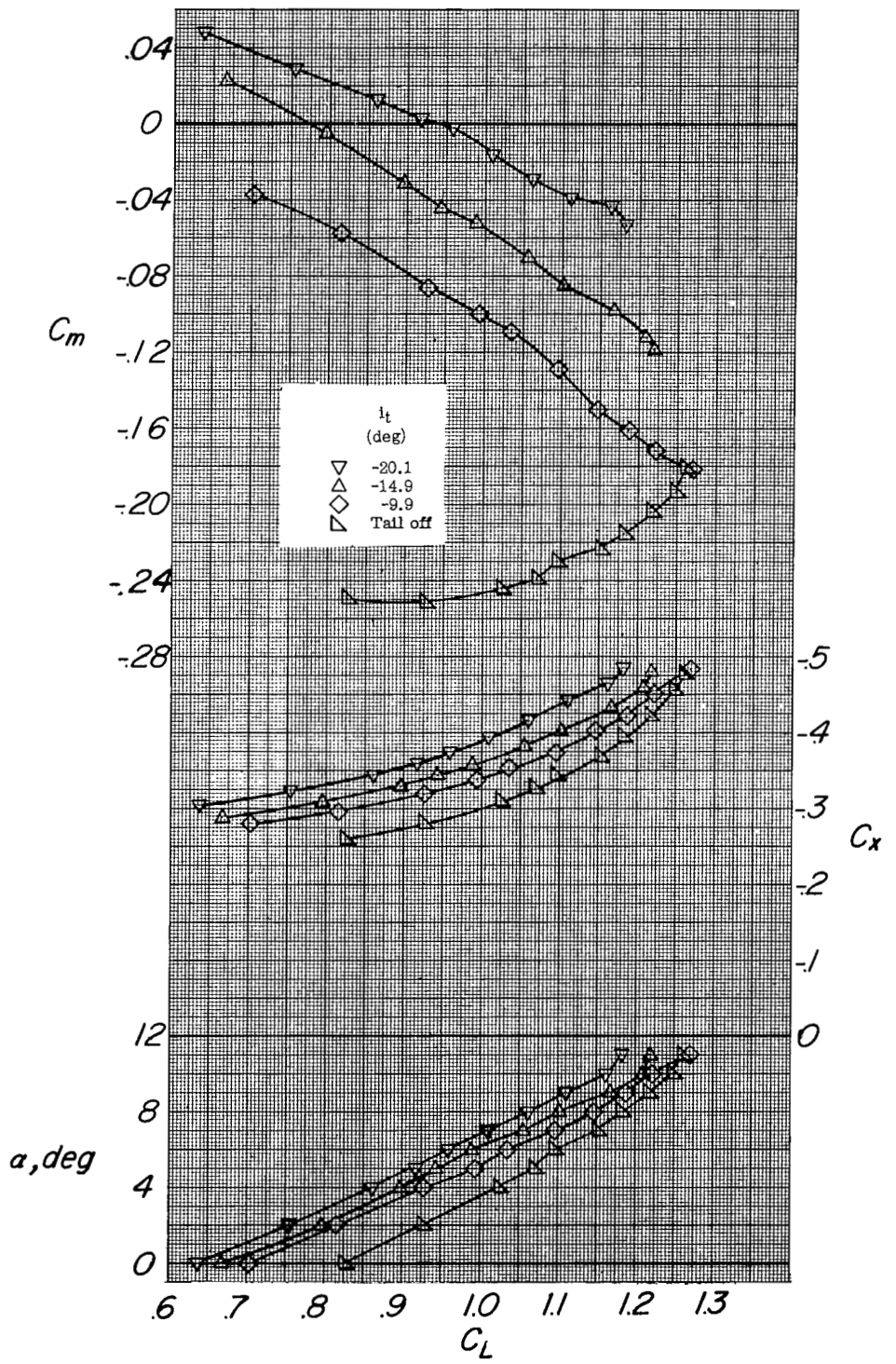

(b) Tanks off; brakes on.

Figure 29.- Continued.

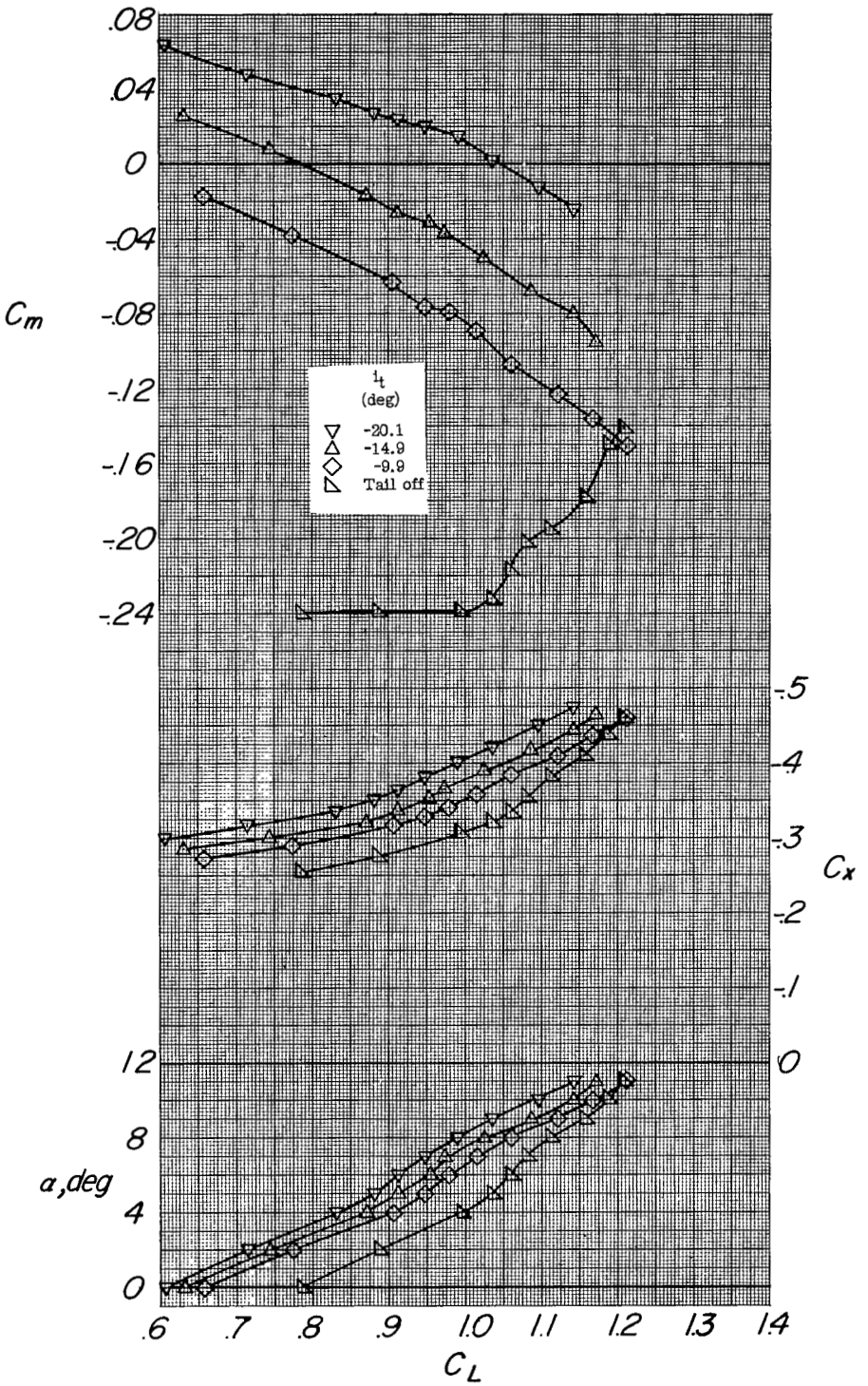

(c) Tanks-33; brakes on.

Figure 29.- Continued.

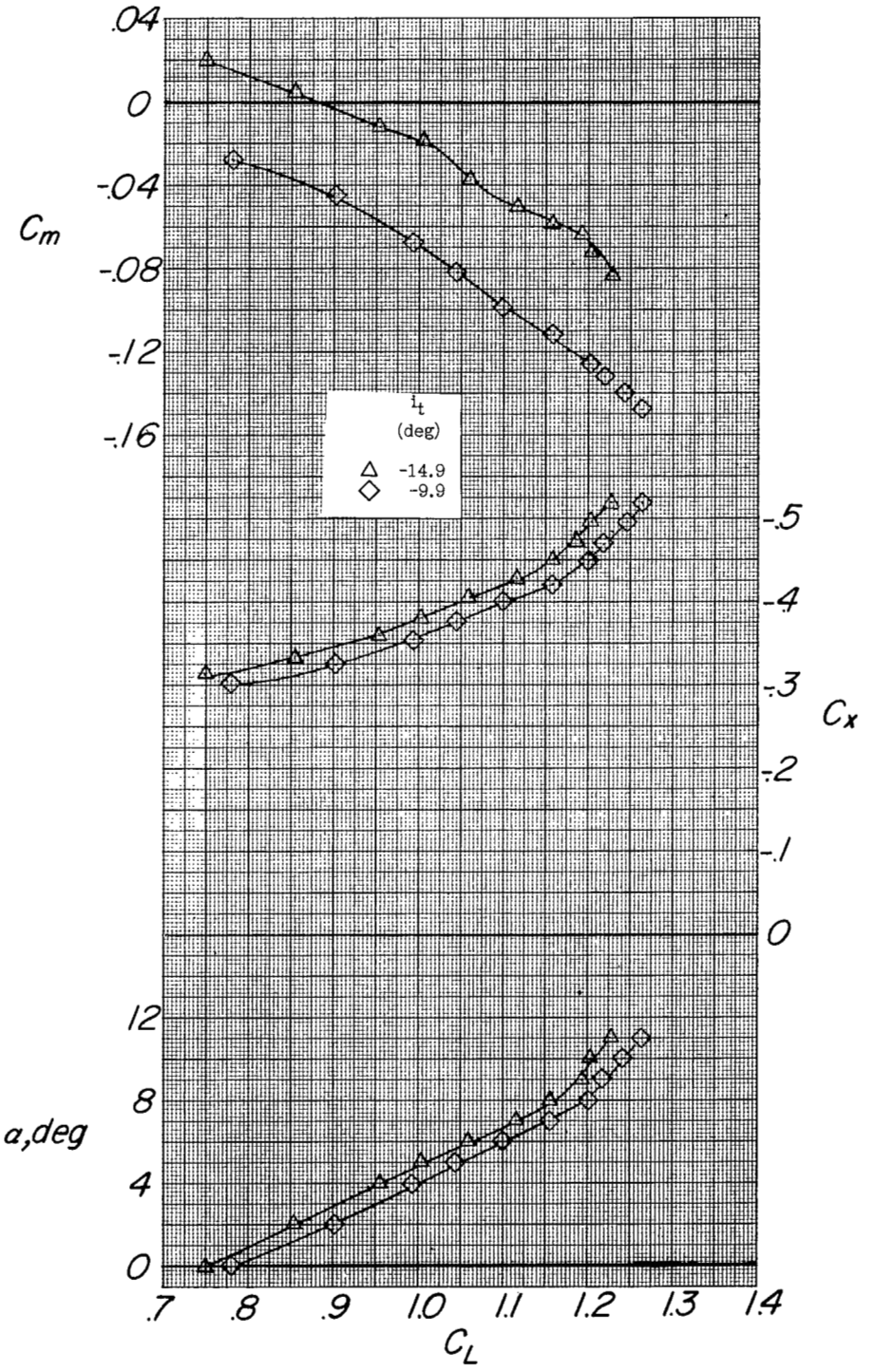

Figure 31.- The effect of the horizontal stabilizer on the aerodynamic characteristics in pitch. Configuration FWVH; $i_w = 2^\circ$; $\delta_f = 50^\circ$; small notch; brakes on; ground board H = 12.5 in.; q = 52.5 lb/sq ft.

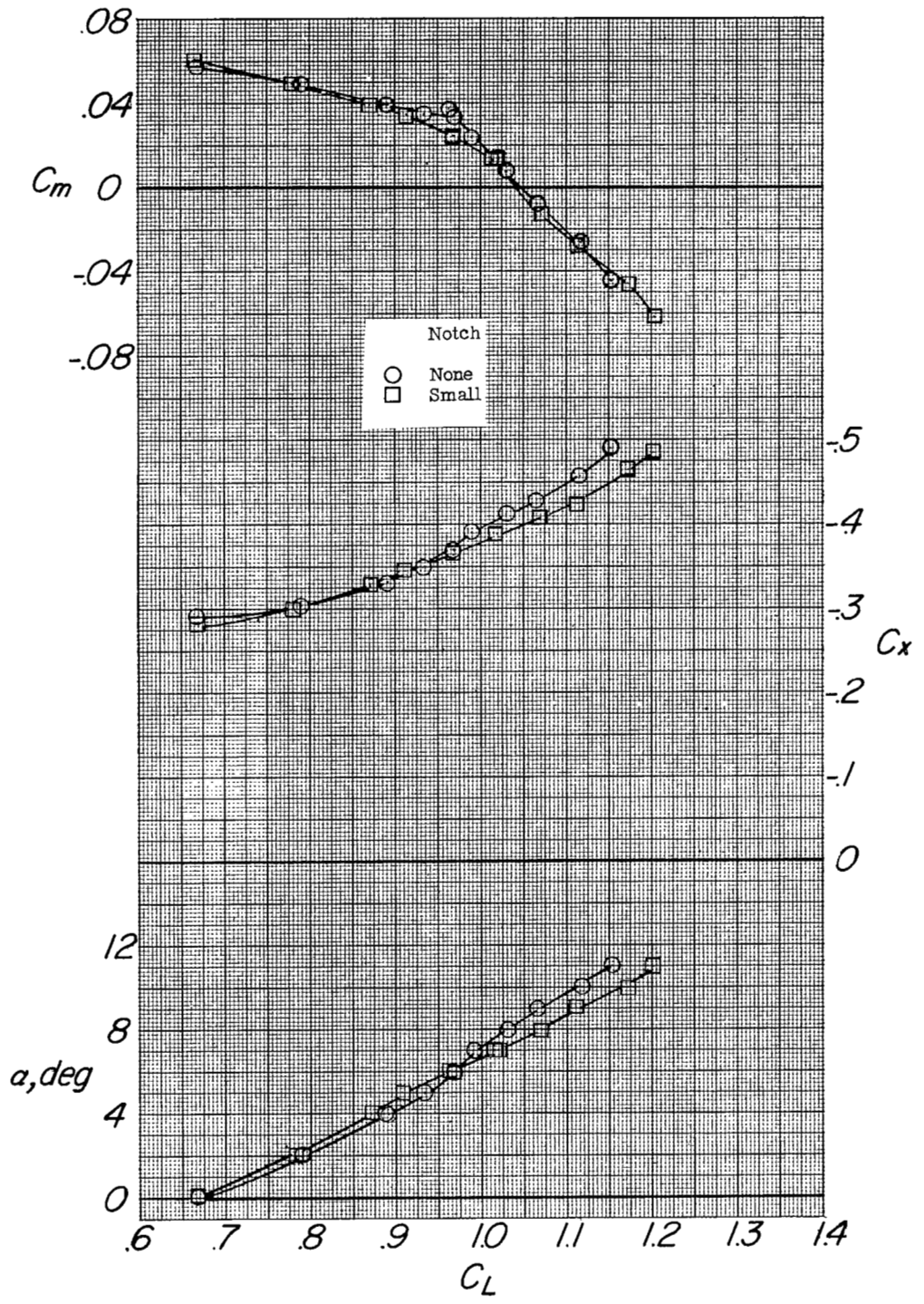

Figure 32.- The effect of leading-edge configuration on the aerodynamic characteristics in pitch. Configuration FWVH; $i_w = 2^o$; $\delta_f = 43^o$; tanks-33; brakes on; ground board H = 12.5 in.; q = 52.5 lb/sq ft; $i_t = -14.9^o$.

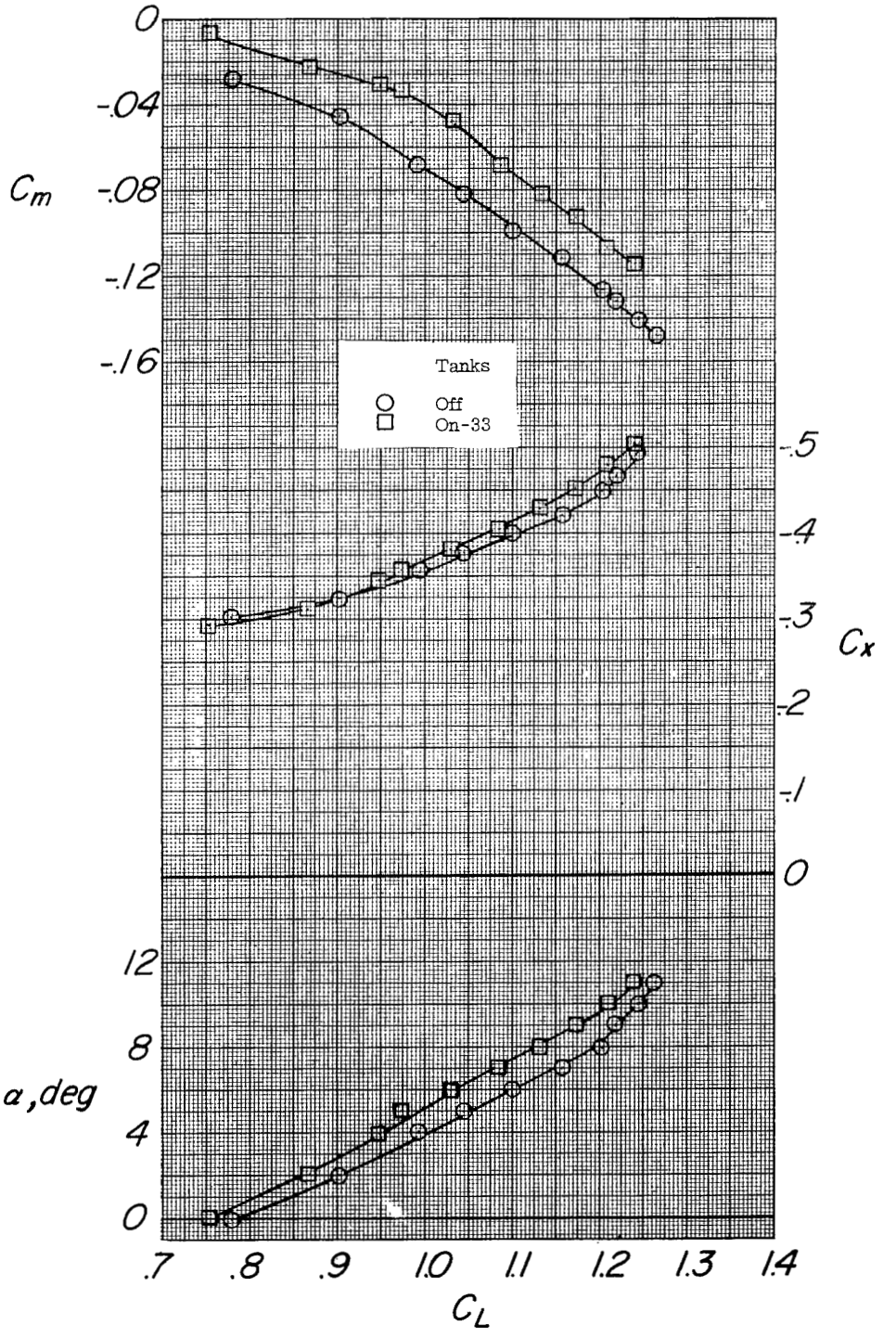

Figure 33.- The effect of tanks on the aerodynamic characteristics in pitch. Configuration FWVH; $i_w = 2^o$; $\delta_f = 50^o$; brakes on; small notch; $i_t = -9.9^o$; ground board H = 12.5 in.; q = 52.5 lb/sq ft.

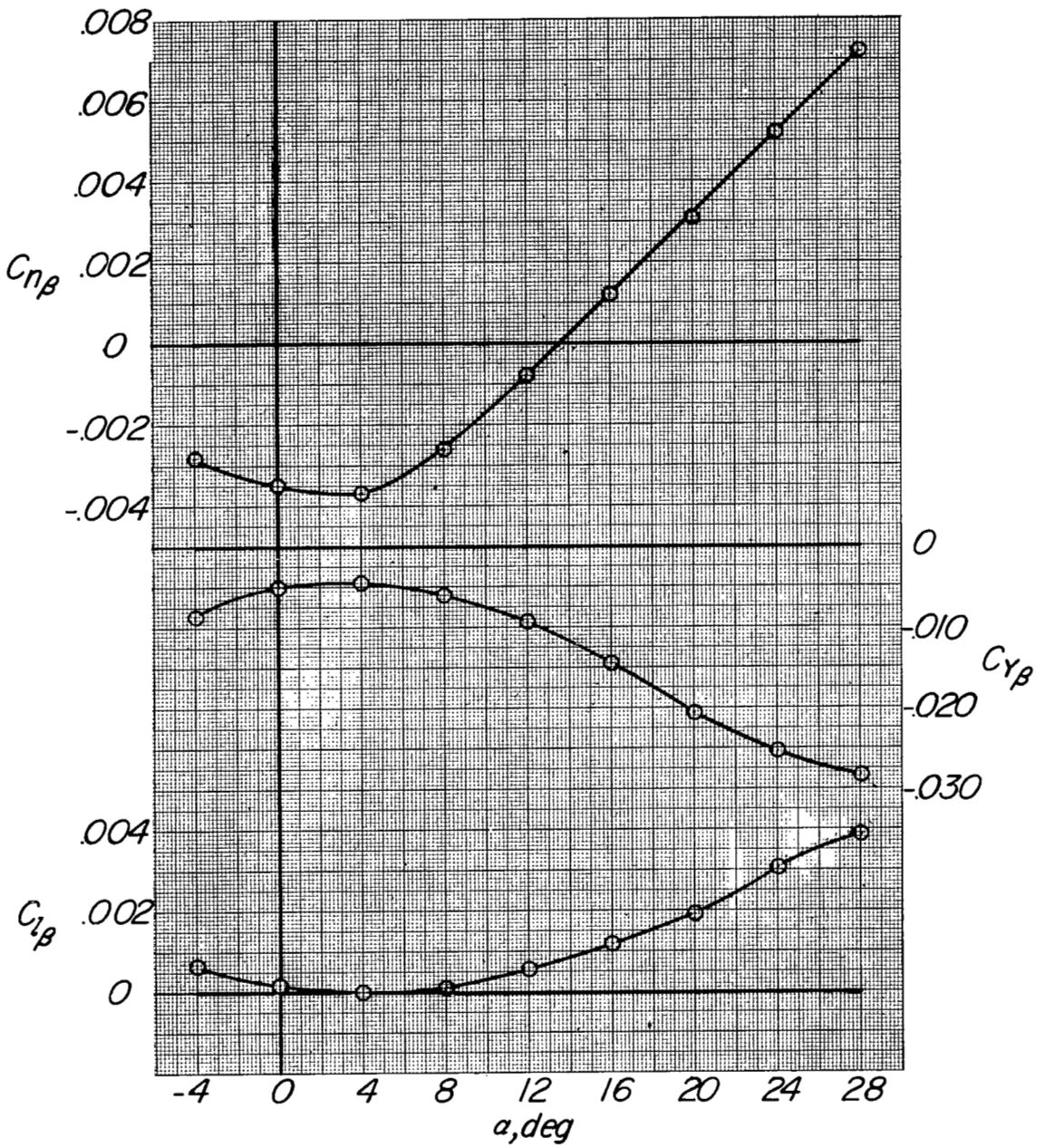

Figure 34.- The variation of the lateral stability parameters with angle of attack. Configuration F; q = 49 lb/sq ft.

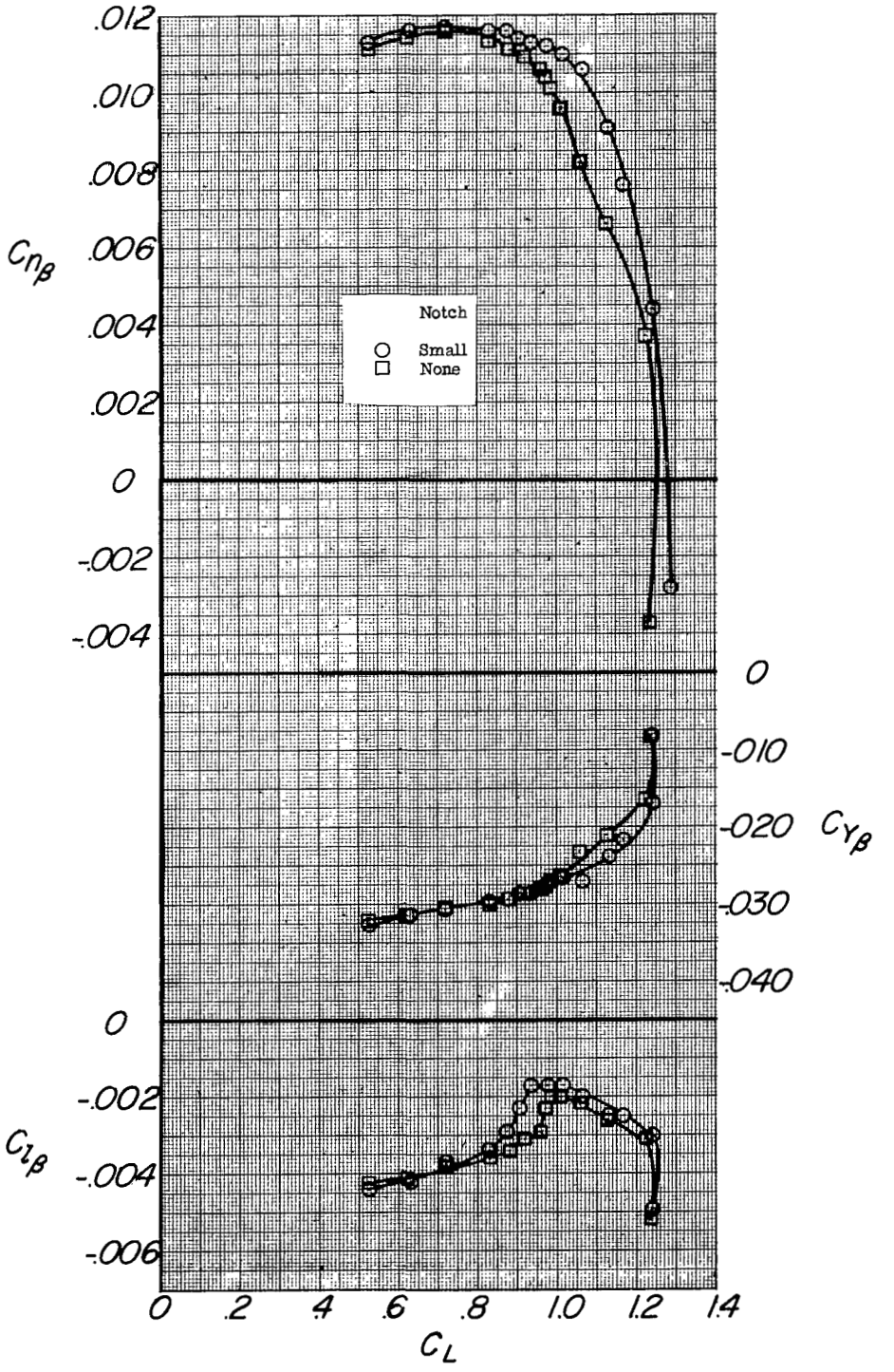

Figure 35.- The effect of leading-edge configuration on the lateral stability parameters. Configuration FWVH; $i_w = 0^\circ$; $\delta_f = 50^\circ$; $i_t = -9.9^\circ$; q = 49 lb/sq ft.

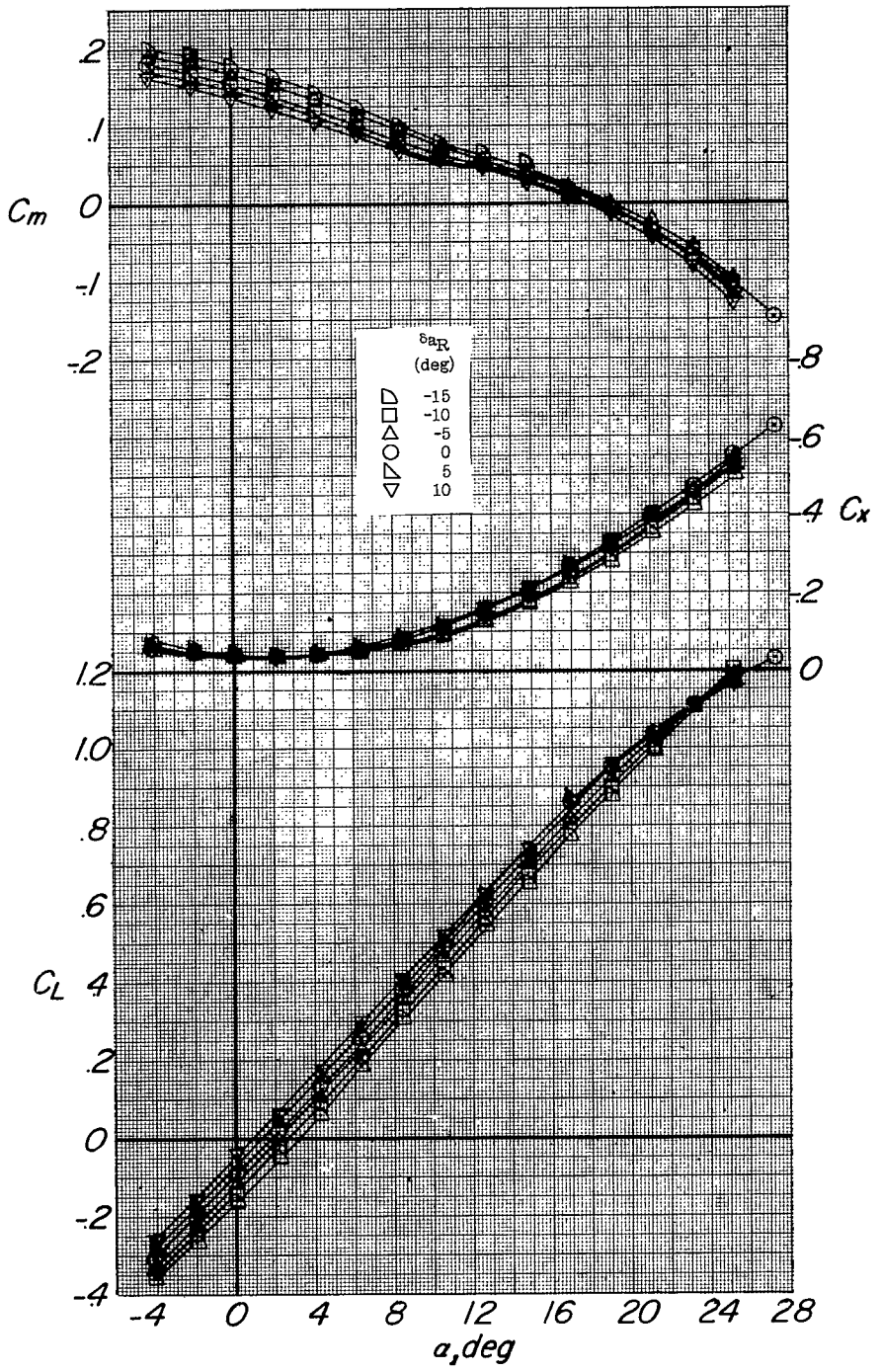

(a) $\delta_f = 0^\circ$.

Figure 36.- The effect of aileron deflection on the aerodynamic characteristics in pitch. Configuration FWVH; $i_w = 0^\circ$; $i_t = -9.9^\circ$; small notch; fence E-33; q = 41 lb/sq ft. Stability tunnel results.

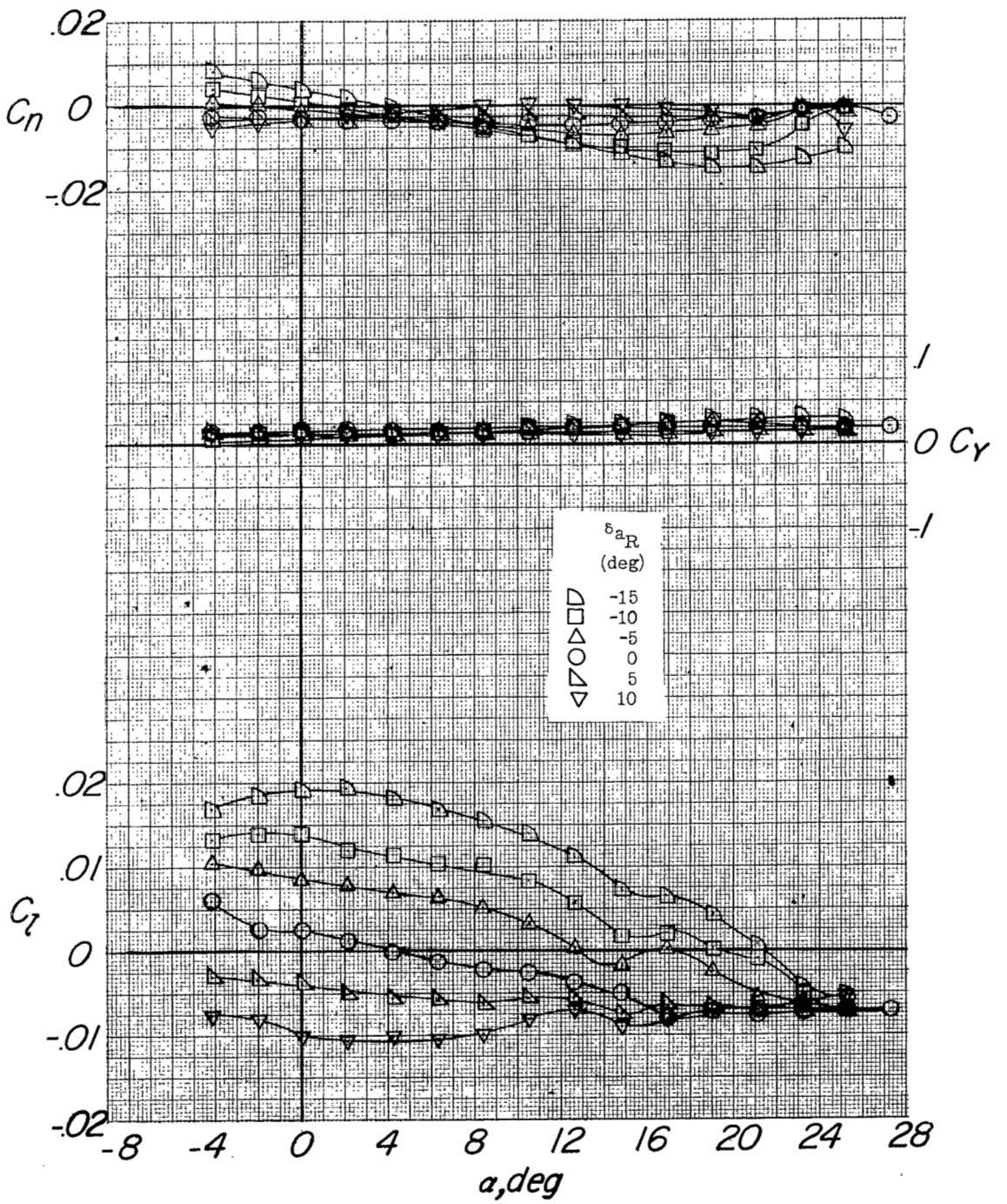

(a) Concluded.

Figure 36.- Continued.

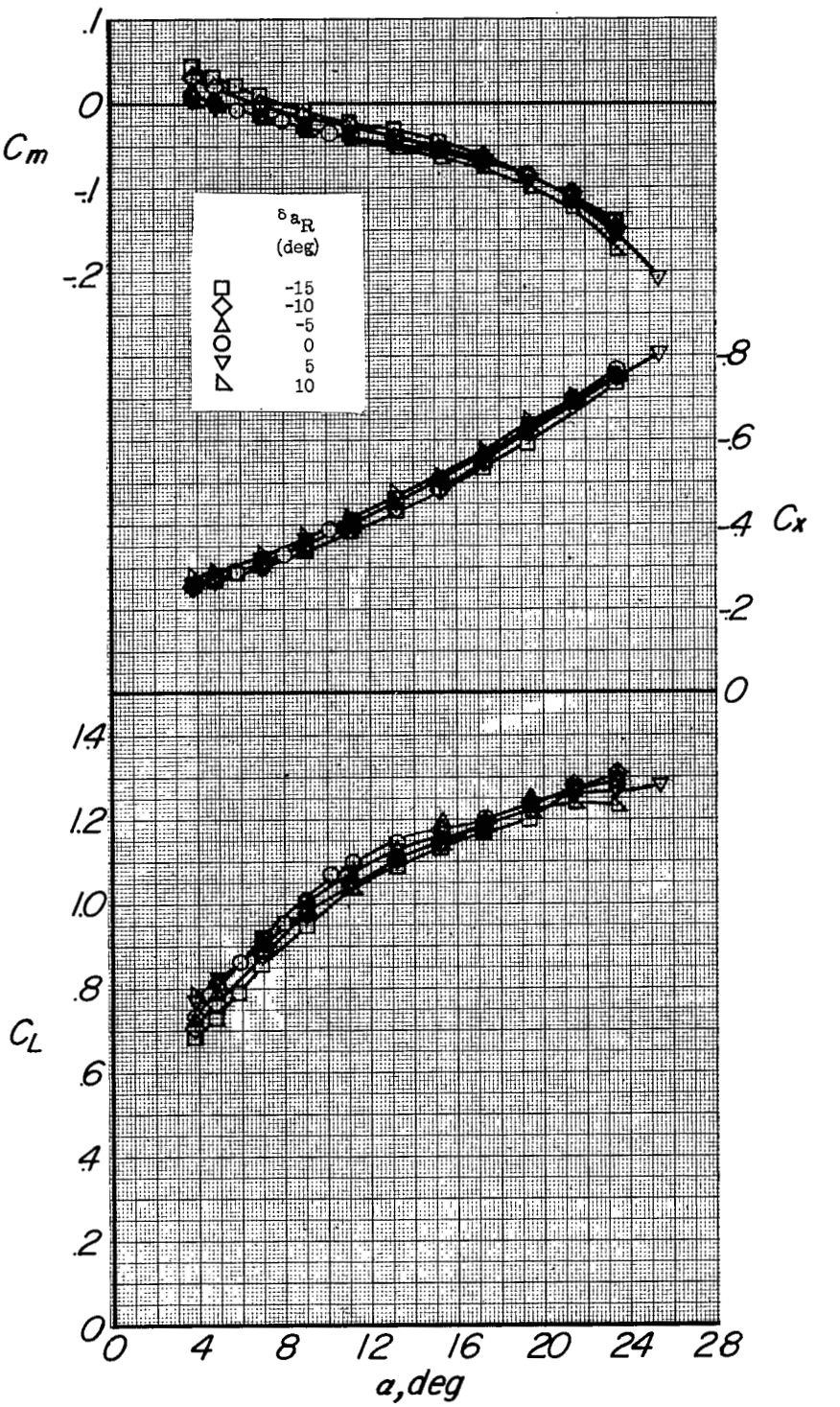

(b) $\delta_f = 50^\circ$.

Figure 36.- Continued.

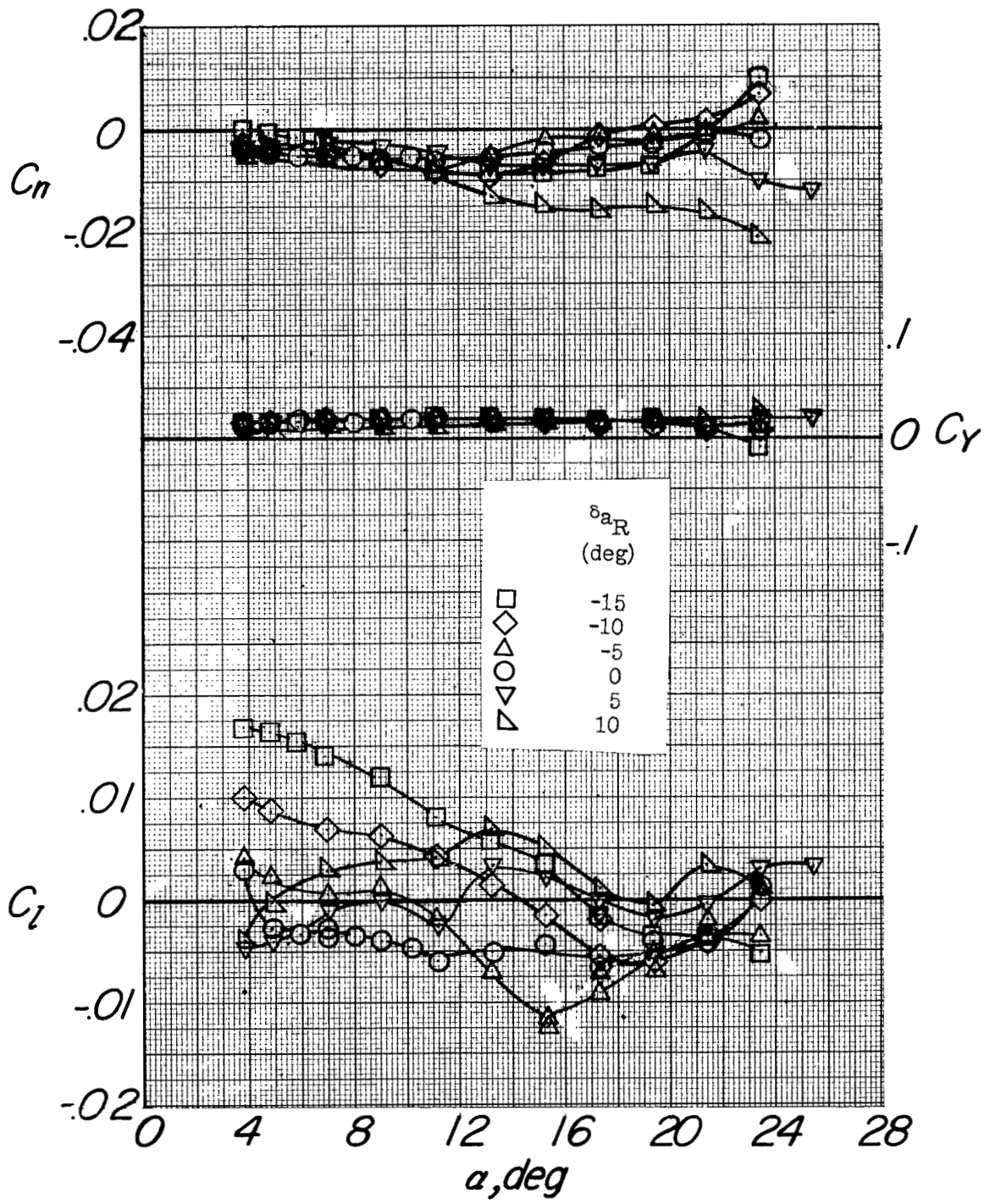

(b) Concluded.

Figure 36.- Concluded.

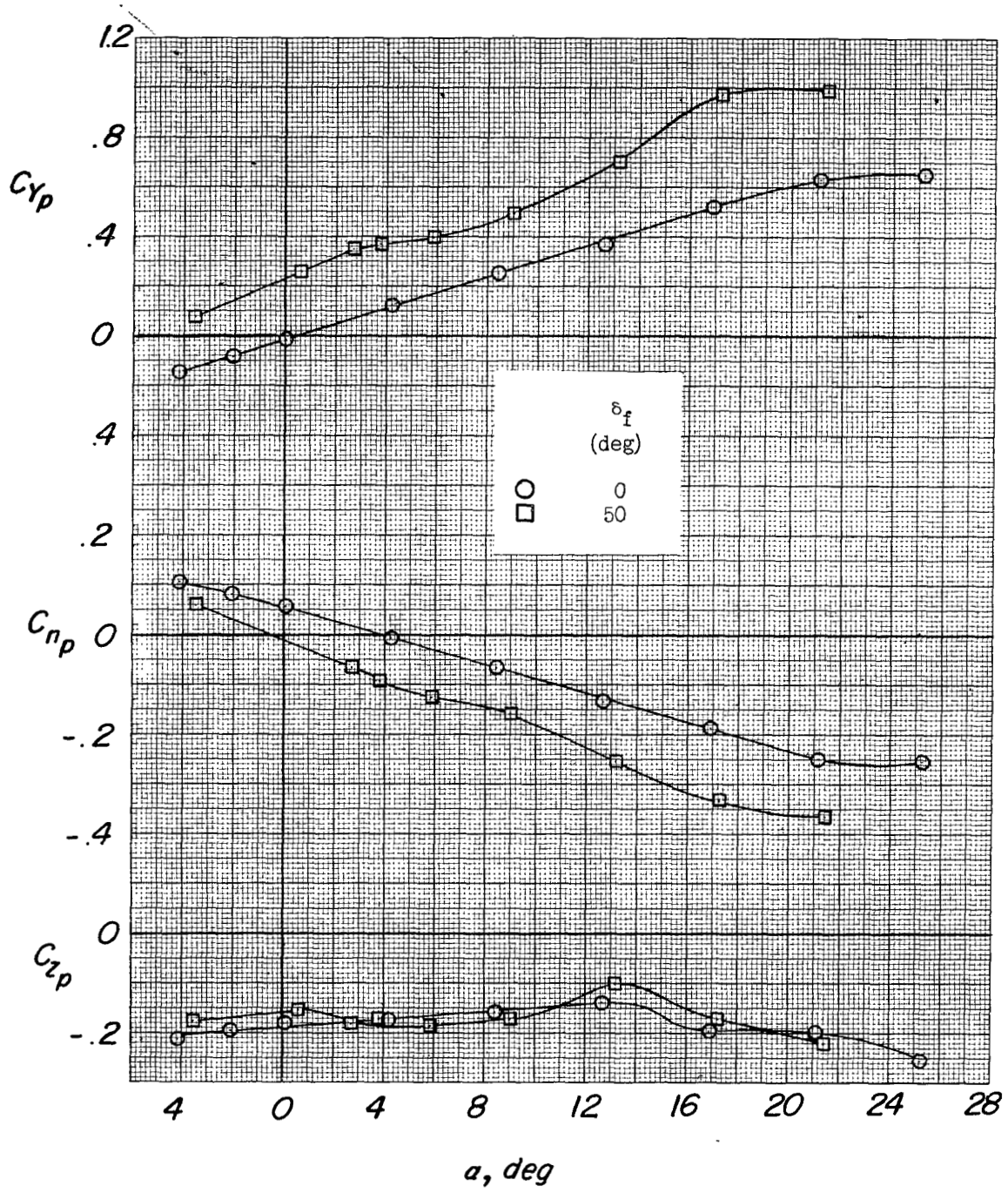

Figure 37.- Variation of the rotary stability derivatives with angle of attack for the high-speed and landing configuration. $i_w = 0°$; $i_t = -10°$; small notch; fence E-33.